TOWARD TWO-DIMENSIONAL MAGNETISM: SINGLE LAYER AND MULTILAYERED FILMS OF TRANSITION METAL ORGANOPHOSPHONATES PREPARED AT LANGMUIR-BLODGETT ORGANIC TEMPLATES

By

HOUSTON BYRD

A DISSERTATION PRESENTED TO THE GRADUATE SCHOOL
OF THE UNIVERSITY OF FLORIDA IN PARTIAL FULFILLMENT
OF THE REQUIREMENTS FOR THE DEGREE OF
DOCTOR OF PHILOSOPHY

UNIVERSITY OF FLORIDA

1994

ACKNOWLEDGEMENTS

I would like to thank my research advisor, Dr. Daniel R. Talham, for all his guidance and patience. I believe that none of what I have accomplished here would have been possible without him. I would also like to thank the members of Dr. Talham's research group for all their support. Margaret Showalter deserves a special thanks for setting up the lab and synthesizing the phosphonate molecules. A very special thanks goes to John K. Pike who analyzed all of my films by XPS. He has been a vital part of this research and a good friend for the past five years.

I would like to acknowledge the Major Analytical Instrumentation Center for the use of the XPS and TEM instruments and thank Mr. Eric S. Lambers and Dr. Augusto A. Morrone.

I would like to thank the National Science Foundation, the UF Division of Sponsored Research, the donors of the Petroleum Research Fund, and the UF College of Liberal Arts and Sciences for financial support during my graduate studies.

I am grateful to Dr. James D. Fisk at Samford University. His constant encouragement and his confidence in me led me to pursue a career in chemistry. I also thank my family, who have shown love, respect and guidance to me all of my life. It is through their encouragement that I have been successful. Finally, I would like to thank my wife, Jill, for being everything I could ever want in a friend.

TABLE OF CONTENTS

page

Abstract of Dissertation Presented to the Graduate School
of the University of Florida in Partial Fulfillment of the
Requirements for the Degree of Doctor of Philosophy

TOWARD TWO DIMENSIONAL MAGNETISM: SINGLE LAYER AND MULTILAYERED FILMS OF TRANSITION METAL ORGANOPHOSPHONATES PREPARED AT LANGMUIR-BLODGETT ORGANIC TEMPLATES

By

Houston Byrd

April 1994

Chairman: Daniel R. Talham
Major Department: Chemistry

Single-layer and multilayer films of zirconium octadecylphosphonate are prepared by the Langmuir-Blodgett technique. An LB template of octadecylphosphonic acid is formed, and then Zr^{4+} ions are "self assembled" from solution. A capping octadecylphosphonic acid LB monolayer is added to complete the bilayer. Transfer ratios ranging between 1:1 and 1:2 and contact angles of 112° indicate that continuous films are prepared. Infrared analysis indicates that an all-trans close packed template is formed and that this organization is retained in the bilayer and multilayer film. X-ray photoelectron spectroscopy (XPS) analysis of the LB template shows a 1:1 ratio of Zr:P, while bilayer and multilayer films possess a Zr:P ratio of 1:2 consistent with the bulk zirconium phosphonate. Ellipsometry shows a linear increase in film thickness.

while X ray diffraction reveals a d-spacing of 52 Å demonstrating the layered nature of the films

Organophosphonate monolayer and multilayer films are prepared by self-assembly at a zirconium-octadecylphosphonate LB template. Octadecylphosphonic acid self-assembled at the LB template produces a close-packed well-ordered bilayer. XPS analysis shows that the bilayer possesses a Zr:P ratio of 1:2. Multilayer films of 1,10-decanediyldiphosphonic acid are also assembled at the zirconated LB template. The fwhm of the $\nu_a(CH_2)$ band indicates that close-packed films are not produced. The rigid α,ω-diphosphonic acid quaterthiophenediphosphonic acid (QDP) is assembled layer-by-layer at the LB template as shown by UV-vis analysis. X-ray diffraction from 10 layers of QDP reveals a d-spacing of 20.19 Å, demonstrating the layered nature of the film.

Manganese octadecylphosphonate films are prepared by LB vertical deposition methods. Infrared analysis of the layers indicates that a close-packed, well-ordered film is produced. XPS analysis reveals a 1:1 Mn:P stoichiometry. Transmission electron diffraction shows that the film possesses an orthorhombic unit cell. The d spacings are identical to those observed in the solid-state analog manganese phenylphosphonate. Electron paramagnetic resonance of the LB films shows evidence for antiferromagnetic exchange and short range antiferromagnetic order in a two dimensional Heisenberg antiferromagnet.

CHAPTER 1
INORGANIC MONOLAYERS AT LANGMUIR-BLODGETT AND SELF-ASSEMBLED ORGANIC TEMPLATES

Low-Dimensional Inorganic Materials

The quasi-two-dimensional structure of layered inorganic solids[1-4] makes them attractive experimental models for investigating chemistry and physics in the limit of two dimensions. These structures are termed "quasi" because although the structures are anisotropic, they are still part of a three-dimensional crystal. In order to investigate true monolayers, single layers of atoms[5,6] and inorganic solids have recently been prepared on surfaces by either chemical vapor deposition or molecular beam epitaxy. However, these films often suffer as two-dimensional models because interactions between the substrate and the monolayer can dominate the physical properties of interest.[7] A different approach to creating a true monolayer is to incorporate two-dimensional arrays of inorganic ions or complexes into organic monolayers that have been formed by Langmuir-Blodgett[8-12] (LB) or organic self assembly[12-14] (SA) techniques. In this chapter we will discuss how organic templates might be used to produce single layers of well-known solid-state inorganic materials.

The Langmuir-Blodgett Technique

The Langmuir-Blodgett (LB) technique is a method used to form monolayer films at an air/water interface. The technique is named for Irving Langmuir[9], who is considered to be the founding father of floating monolayer research, and Katharine Blodgett[8], who is credited with transferring monolayers

from the air/water interface onto solid supports. Although the LB method was developed in the early 20th century, only a handful of researchers pursued this area of research until the mid-1970s when the first automated LB trough was developed. Automation of the LB technique brought about a renewed interest in this method.

Langmuir Monolayer

In order to prepare a monolayer at the air/water interface, the molecules must spread when placed on the water surface. The force that causes molecules to spread can be described as surface tension γ which is expressed as

$$\gamma = (\delta G/\delta s)_{T,P,n} \qquad (1\text{-}1)$$

where G is the Gibbs free energy, s is surface area, and temperature T, pressure, P, and the number of moles, n, are held constant. The classic monolayer forming materials possess two distinct regions[10,12]: a hydrophilic headgroup and a hydrophobic tail. The headgroups are immersed in the water while the tails remain outside of the water. These types of molecules are termed amphiphilic molecules, and when these molecules are placed on a water surface, they spread to cover all of the available area. Once the molecules are placed on the water subphase, they can be compressed into a close-packed film by a movable barrier.

A Langmuir monolayer is usually formed in a PFTE (teflon) coated trough that possesses movable barriers (Figure 1-1), which are used to compress the molecules into a close-packed film. The packing of the molecules is monitored

by the change in the surface tension at the interface which is defined as surface pressure π

$$\pi = \gamma - \gamma_0 \qquad (1\text{-}2)$$

where γ is the surface tension in the absence of a monolayer and γ_0 is the surface tension when the monolayer is present [18]

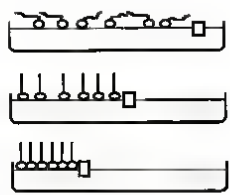

Figure 1-1 A floating Langmuir monolayer

The surface pressure (units are mN/m) is measured by a Wilhelmy balance [18] When the compression is carried out at constant temperature it is called a pressure/area isotherm (π/A) Figure 1-2 is an isotherm of stearic acid on a pure water subphase In this isotherm three distinct regions are observed the "gas analogous" "liquid analogous" and "solid analogous" regions [10 12] While in reality these three "analogous" classification are often more complicated they are helpful in understanding monolayer formation and aid in gaining information about the molecules The first region is termed "gas

analogous" because upon spreading of the molecules, there is little interaction between the molecules. In the isotherm no change in surface pressure is observed in this region. As the film is compressed, the molecules start to interact and the pressure begins to increase; this region is then referred to as the "liquid analogous" region. Finally, when the molecules are close packed, the pressure increases rapidly, and this is referred to as the "solid analogous" region. In the solid analogous region, the cross-sectional area per molecule in the close-packed film can be determined. The cross-sectional area is obtained by extrapolating the slope of the sharp increase in pressure to zero pressure. At this point, the molecules are close-packed, and knowing the total number of molecules compressed in this area leads to the area per molecule. For stearic acid, the cross-sectional area on a pure water subphase is 20.01 $Å^2$.[10,12] The sharp decrease in pressure at the apex of the isotherm is the point where the film collapses. It is believed that at this point the film folds over on itself, and a monolayer no longer exists at the air/water interface.

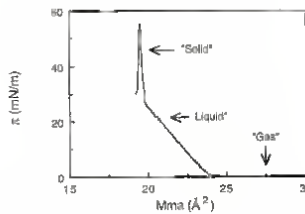

Figure 1.2. Pressure/area isotherm of stearic acid compressed on a pure water subphase.

Langmuir-Blodgett Method

In 1919 the first fatty acid was transferred to a solid support from the air water interface [8]. Katharine Blodgett, who joined Langmuir's research group in 1919, is given the credit for developing this method. The basic method (Figure 1-3) for transferring monolayers involves a substrate such as a glass slide, being drawn up through the air/water interface while a specific surface pressure in the solid analogous region is maintained. As the substrate passes through the air/water interface, the head groups of the molecules physisorb to the surface. Continued deposition of the substrate through the floating monolayer produces a multilayered film. One of the advantages of the LB method is that the number of transferred layers can be easily controlled. This enables film thicknesses to range from a monolayer to hundreds of layers [10-12]. In most cases, the transfer occurs at pressures that range from 15-30 mN/m. If the pressure is too low upon transfer the molecules are not close packed, which results in disorganized films. If the pressure is too high, the film becomes too rigid. In either case transfer of the floating monolayer is difficult.

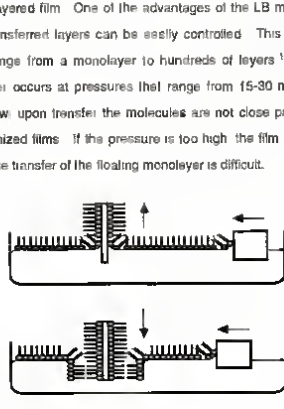

Figure 1-3. Langmuir-Blodgett deposition.

There are three classes[10-12] of LB films that can be produced on solid supports. The first, and the most common, is called Y type deposition (Figure 1-4). This is where the monolayer transfers on both the upstroke (head-to-head transfer) and the downstroke (tail-to-tail transfer). The two other types of deposited films are X-type, where the film only transfers on the downstroke (tail-to-head transfer) and Z-type, where the film only transfers on the upstroke (head-to-tail transfer).

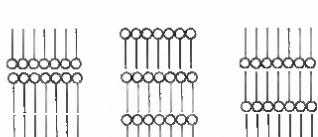

Figure 1-4 The three types of transferred LB films

In discussing transferred films, it is necessary to introduce the concept of the transfer ratio. The transfer ratio is a means by which the quality of deposited LB films are monitored in real time. The transfer ratio[10-12] (TR) is defined as

$$TR = A_f / A_s \qquad (1\text{-}3)$$

where A_f is the decrease in area occupied by the monolayer (at constant pressure) and A_s is the area of the substrate that is pulled through the floating monolayer at the air/water interface. For complete coverage of the substrate by the monolayer, the transfer ratio should be equal to 1. Figure 1-5 demonstrates the transfer of stearic acid to a glass slide. One parameter that is monitored

during the deposition is the barrier movement. For a successful deposition, the barrier movement should be a straight line possessing a slope of 1. The linearity of the transfer can be used as a real time measure of the quality of deposited films. A linear barrier movement indicates that a continuous film has been deposited. A nonlinear barrier movement would indicate that the substrate possesses regions where the film did not transfer.

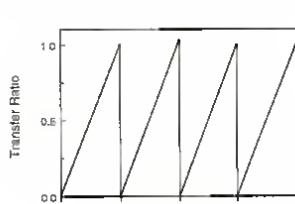

Figure 1-5. Transfer ratio for stearic acid deposited onto a glass slide.

The Langmuir-Blodgett method is not only useful for preparing organic thin films but can be used as an organic host or template to prepare single layers of inorganic ions. It is well known that metal ions in solution can interact with the LB film at the air/water interface under the proper conditions[10-12] (Figure 1-6). In the case of carboxylic acids, if the pH > 5.5 the acid will begin to ionize and will bind cations (e.g. Ce^{2+}, Ba^{2+}, Na^{+} etc.) from solution. These ions, once incorporated into the films, will remain even upon transfer of the films to solid supports. Transferred LB films have been used for a large variety of

applications. Some of the areas of interest are optical devices, insulators for semiconductor devices and sensors [11]

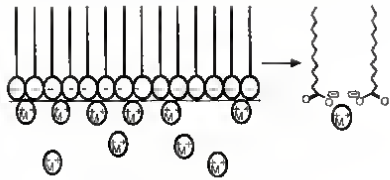

Figure 1-6 Metal-ion incorporation at the air/water interface

Inorganic Monolayers Prepared at LB Templates

The use of organized Langmuir-Blodgett monolayers to prepare inorganic particles is currently an area of interest. One approach is to use a floating monolayer as a site of nucleation and grow crystals of inorganic solids from the subphase. This method has been useful in preparing oriented inorganic crystals of materials such as $BaSO_4$ [15,16] $CaCO_3$[17,18] and PbS_2 [20]. In these studies selected crystal morphologies and preferred orientations have been achieved. However, only three-dimensional crystals have been prepared using this technique. Our hypothesis is that the LB method can be used to prepare single-layer analogs of known solid-state materials by incorporating an inorganic monolayer into the LB film at the air/water interface. Transferring a Y-type bilayer of this newly formed inorganic/organic monolayer to a solid support would result in a single layer of an inorganic extended lattice system. This concept is illustrated in Figure 1.7 and is discussed in the next few chapters.

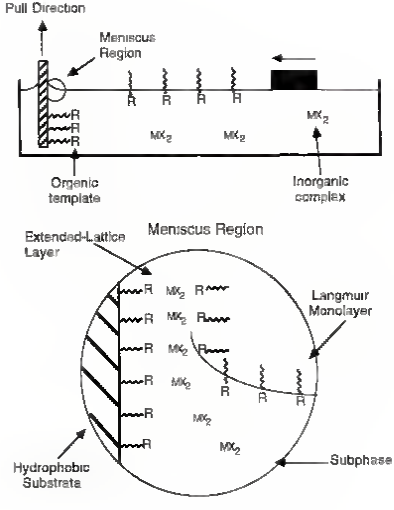

Figure 1-7 Idealized deposition procedure for the formation of single-layer extended-lattice inorganic systems

Self-Assembly

Self-assembled (SA) monolayers are formed from molecules that spontaneously chemisorb at an appropriate substrate when the substrate is immersed into a solution containing these functionalized molecules (Figure 1-6). There are several types of molecules that have been shown to self-assemble to surfaces. These include organosilanes[13-21] alkanethiols[12,14,22] and carboxylic acids.[12] The organosilanes are known to adsorb onto hydroxylated surfaces such as SiO_2 or Al_2O_3, while the alkylthiols will assemble on gold, silver or copper surfaces, and the carboxylic acids will assemble onto aluminum oxide or silver surfaces. The first example of self-assembly was reported by Zisman and coworkers[21] in 1946. Since then, basic research on SA films has been carried out by many researchers. For example, Sagiv[13] Whitesides[14,22] and Ulman[12] have studied the chemistry and energetics of self assembly.

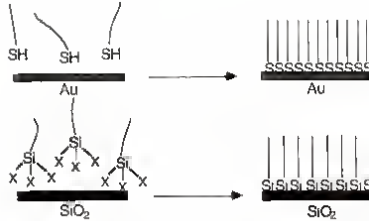

Figure 1-6. Self-assembly of an organosilane to a SiO_2 substrate and an alkylthiol to a Au substrate

According to Ulman [12] the energetics of the self-assembly of molecules can be divided into three parts (Figure 1 9) The first part involves the functional group or head group that chemisorbs to the surface This is the most exothermic process in self-assembly It is accepted that a chemical bond is formed between the head group and the substrate For example in the case of the organosilanes a Si-O bond is formed while a S-Au bond is formed in the case of the alkylthiols adsorbed to gold The energies of the bond formation is on the order of tens of kcal/mol and for the thiols this is 40-45 kcal/mol [12]

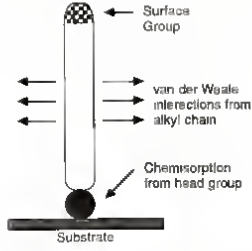

Figure 1-9 The energetics involved in the self-assembly of molecules

The second contribution to the energy of adsorption is associated with the packing of the alkyl chains of the molecules The van der Waals interactions that are associated with the alkyl chains are on the order of a few kcal/mol It is only after the head groups adsorb that the van der Waals interactions play an important role The van der Waals interactions are responsible for the packing

end order of the alkyl chains. The final part involves the terminal functionalities which are thermally disordered at room temperature.

Most of the research on SA films has been confined to the study of monolayers. However, there are a few methods that have been used to prepare multilayered films via self assembly. The first report of multilayer films prepared by organic self-assembly was published by Sagiv and coworkers.[23] In this procedure, a monolayer of 15-hexadecenyltrichlorosilane (HTS) is adsorbed onto an oxide surface followed by activation of the terminal olefin to produce a surface of hydroxyl functionalities (Figure 1.10). The OH terminated surface can adsorb another layer of HTS, and by repeating the process multilayer films can be constructed. However, after the first few layers structural defects began to form in the films. Also in this procedure, questions were raised concerning the extent of the conversion from the terminal functional group to hydroxyl groups. In an attempt to overcome these shortcomings, Mallouk and coworkers[2,24-27] developed a technique for one-layer-at-a-time self-assembly of transition metal phosphonates. This procedure is detailed in the next section.

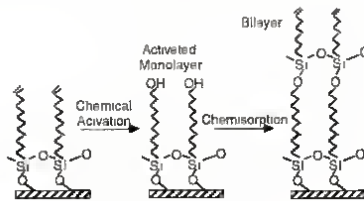

Figure 1.10. The first report of multilayer films prepared by organic self-assembly of 15-hexadecenyltrichlorosilane (HTS).

Procedures have been developed where self-assembled organic layers are linked by transition metal ions [2,24,25]. Mallouk and coworkers[2,24,27] demonstrated a self-assembly method for one layer at a time depositions of transition metal phosphonates. In the solid state the transition metal phosphonates are layered structures in which the metal ions and phosphonate groups reside in sheets (Figure 1-11). The bonding within the metal ion plane is thought to be independent to the nature of the organophosphonate group. The thermodynamic stability and extreme insolubility of the transition metal phosphonates allowed Mallouk to prepare self assembled thin films of the phosphonates.

In this procedure (Figure 1-12) a molecule bearing two functionalities such as a thiol at one end and a phosphonate group at the other end is adsorbed to a substrate. This self assembly procedure produces a thin film with a phosphonic acid terminated surface. Transition metals are then assembled from solution to the phosphonic acid molecules. Multilayers are constructed by alternately adsorbing α,ω–diphosphonic acid molecules and metal ions from solution.

Multilayered films have been produced with tetravalent[24,25,27,28] (Zr^{4+} and Hf^{4+}) trivalent[26] (Y^{3+}) and divalent[30] (Zn^{2+} and Cu^{2+}) transition metals. Mallouk and coworkers[30] have also varied the length of the diphosphonic acid alkyl chain ($H_2O_3P(CH_2)_nPO_3H_2$ n = 6, 8, 10, 12, 14). They have demonstrated that the films are deposited one layer at a time and by automating the deposition process have routinely produced films with 100 or more layers. These films are considered to be relatively pinhole free and act as insulators in metal-insulator-semiconductor and metal-insulator-metal sandwich devices.[29] However, grazing angle X ray diffraction from planer surfaces has not been

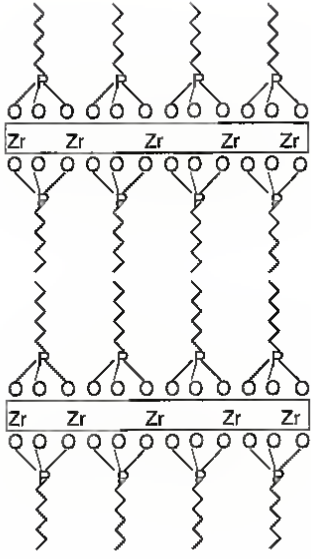

Figure 1-11. Zirconium phosphonate layered solid state structure

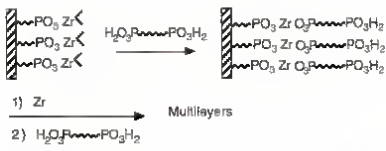

Figure 1-12 Deposition scheme for zirconium phosphonate multilayers

observed in these materials. There is also no conclusive evidence to suggest that the films are well ordered.

The question of order within the films arises from the initial phosphonic acid layer or template layer. In the published procedures, the initial layers are prepared from 3 (hydroxyldimethylsilyl)-propyl phosphonic acid[24,25] deposited on oxide surfaces or the disulfide $[S(CH_2)_4PO_3H_2]_2$ deposited on gold surfaces.[25] Neither of these initial layers is expected to produce a well-ordered layer. While Mallouk's method was developed as a way to produce multilayered films and he has been successful in this approach, our objective is to prepare single-layer analogs of known solid-state materials. We propose that in order to prepare an organized single layer of an extended-lattice solid-state material, a well-ordered template is essential. Therefore, in the next few chapters we will discuss how the LB technique, which produces well-ordered films, can be used as a method for preparing single-layer and multilayered films of the thermodynamically stable transition metal phosphonates. We will show that well-ordered films can be produced by this method and that low-dimensional magnetic materials can also be prepared.

CHAPTER 2
INORGANIC MONOLAYERS FORMED AT AN ORGANIC TEMPLATE. A LANGMUIR-BLODGETT ROUTE TO MONOLAYER AND MULTILAYER FILMS OF ZIRCONIUM OCTADECYLPHOSPHONATE

Introduction

Current interest in layered inorganic materials ranges from applications in intercalation chemistry,[1] catalysis[1] and separations[2] to the study of superconductivity and magnetism[1,3,4] where the quasi-two-dimensional structure of layered solids makes them attractive experimental models for investigating chemistry and physics in the limit of two dimensions. A potentially better model for two dimensions is a true monolayer, and recent advances in synthesis and characterization at surfaces have led to studies of single layers of atoms[5] or compounds,[6] prepared on surfaces by molecular beam epitaxy or chemical vapor deposition methods. Frequently however these monolayer films suffer as two-dimensional model systems because interactions with the substrate often dominate the physical properties of interest.[7] Another approach to inorganic monolayers is to incorporate two dimensional arrays of inorganic ions or complexes into organic monolayers that have been formed by Langmuir Blodgett[10-12] (LB) or organic self-assembly[12-14,22] (SA) techniques. This approach was first investigated by Pomerantz[31,32] in studies of magnetic ordering in LB bilayers of manganese stearate.

The use of transferred LB films to form single layers, as well as multilayers, of layered zirconium phosphonates is reported here. The method developed here demonstrates the idea of assembling an inorganic monolayer

at a preformed organized organic template (Figure 2-1) and should be useful when applied to other layered systems,[4] including those that can be models for two dimensional magnetism. A feature of these structures is that the inorganic lattice is isolated from the substrate by the organic template layer. When choosing inorganic systems for these studies, we draw on what is known about the structure of the three-dimensional solid-state analogs.[33-35] Our hypothesis is that the best chance to prepare a monolayer of an inorganic extended lattice is to investigate systems such as the metal phosphonates[33-39] that form layered structures in the bulk crystalline phase.

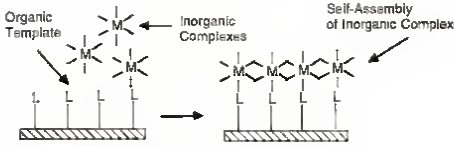

Figure 2-1 Inorganic self assembly of an organic template

Transition metal alkylphosphonates belong to the class of organic-inorganic layer compounds[4] in which layers of inorganic ions are separated by organized organic layers. Examples of the alkylphosphonates have been synthesized with divalent,[36,37] trivalent,[38] and tetravalent metal ions.[33-35] In the tetravalent Zr systems $Zr(O_3PR)_2$, it is thought that the metal-phosphonate binding[34,35,39] is similar to the binding[33] observed in α-$Zr(HPO_4)\cdot H_2O$ where the metal ions are octahedrally coordinated by oxygen atoms with the three oxygens of each phosphonate bound to three different zirconium ions.[33,39]

Each layer consists of a plane of metal atoms linked by layers of phosphonate groups above and below the metal ion plane (Figure 2-2).[33-35] The zirconium phosphonates are extremely insoluble, and Mallouk and coworkers[2,24-27,29] have shown that thin films can be deposited onto surfaces by first anchoring a layer of molecules bearing the phosphonate functionality followed by alternately adsorbing Zr^{4+} ions and α,ω-alkanediyldiphosphonic acid layers from solution. Other groups[40-44] have used this method to prepare oriented assemblies of functionalized molecules one layer at a time for applications such as second harmonic generation.[40-42] In order to form an organized inorganic monolayer, we propose that the key is the first step where the array of phosphonate sites that form the template (Figure 2-1) must be close packed. None of the published methods[2,24-27,29,40,42,45] have resulted in a close packed template layer required to form an organized inorganic monolayer. We have, therefore, investigated the LB technique as a method to form suitable organic template systems for preparing inorganic monolayers.

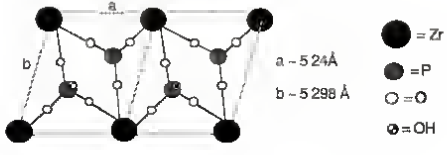

Figure 2-2 Idealized structure of α $Zr(HPO_4)\,H_2O$

Octadecylphosphonic acid forms a film at the air/water interface [45-46] Upon addition of Zr^{4+} ions to the water subphase the octadecylphosphonic acid Langmuir monolayer becomes extremely rigid [45 47] and conventional vertical LB deposition is not possible. Therefore we have developed a new stepwise deposition procedure that involves a combination of LB and "inorganic salt assembly" methods to prepare monolayer and multilayer films of zirconium octadecylphosphonate Characterization of bilayer and multilayer films shows that the structure of these films is similar to that observed for the bulk zirconium phosphonate solids [33-35] In addition the insolubility of the films suggests that the procedure might also be useful for forming stable films of oriented organic molecules

Experimental Section

Materials

Octadecylphosphonic acid ($C_{18}H_{39}O_3P$) was synthesized by Margaret Showalter[45] from commercial octadecylbromide purchased from Aldrich Chemical Co (Milwaukee WI) using the Michaelis Arbuzov[49] reaction followed by acid hydrolysis The acid was recrystallized twice from methanol and dried under vacuum Zirconyl chloride 98% was used as purchased from Aldrich

Substrate Preparation

Single-crystal (100) face silicon wafers purchased from Semiconductor Processing Company (Boston MA) were used as deposition substrates Silicon attenuated-total-reflectance (ATR) crystals 50mm x 10mm x 3mm purchased from Wilmad Glass (Buena NJ) were used as substrates for all

infrared experiments. Silicon ATR crystals were parallelograms with a 45° angle of incidence with respect to the parallel faces. The silicon substrates were cleaned using the RCA cleaning procedure[50] then dried under N_2. Octadecyltrichlorosilane (OTS) coated surfaces were prepared by placing the cleaned substrates in a 2% solution of OTS in hexadecane for 30 minutes and were then rinsed in a chloroform Soxhlet extractor for 30 minutes. Copper transmission electron micrograph grids (400 mesh) purchased from Ted Pella Inc. (Redding, CA) were attached to a glass slide[51] for deposition.

Instrumentation

The Langmuir-Blodgett experiments were performed using KSV instruments (Stratford, CT) Teflon-coated LB troughs with hydrophobic barriers. The surface pressure was measured by a platinum Wilhelmy plate. A Barnstead NANOpure purification system produced water with a resistivity of 18 MΩ-cm for all experiments. Single-barrier pressure versus area (π-A) isotherms were recorded using a KSV 3000 Langmuir-Blodgett instrument, and all depositions were carried out using the KSV 3000 system. Brewster angle measurements were performed on a dual barrier KSV 5000 Langmuir Blodgett trough. In all cases, films were compressed linearly at a rate of 5mN/m/min at room temperature. For the depositions, a target pressure of 20mN/m was maintained with deposition speeds of 10mm/min.

The Brewster angle microscope used was a BAM 1 from Nanofilm Technologie GmbH (Göttingen, Germany). A He-Ne laser was used as the light source and was set at an angle of incidence of 53°. Films were compressed with a dual barrier trough at a linear rate of 5 mN/m/min. The data were recorded by a CCD camera and stored on video tape.

Advancing contact angle measurements were made with a Ramé-Hart (Mountain Lakes, NJ) NRL Contact Angle Goniometer Model 100-00. A 250 mL syringe was used to dispense a fixed-volume water drop to the surface.

Infrared spectra were recorded with a Mattson Instruments (Madison, WI) Research Series-1 Fourier Transform Infrared (FTIR) spectrometer using a narrow-band mercury cadmium telluride detector. A Harrick (Ossining, NY) TMP stage was used for the ATR experiments. All spectra consist of 1000 scans at 4.0 cm^{-1} resolution and are ratioed to the OTS-covered substrates.

Film thickness was measured with a Gaertner (Chicago, IL) Model L117 ellipsometer employing a 70° angle of incidence with a HeNe laser, λ = 632.8 nm, as the source. The refractive index and thickness of the films were calculated from Ψ and Δ using an in-house computer program.

Low-angle X-ray diffraction was performed on the films with a Rigaku 18 kW rotating anode diffractometer. The X-ray source was the Cu Kα line λ = 1.54 Å, which was first passed through a graphite monochrometer. The diffracted X-ray beam was passed through a graphite analyzer before hitting the detector to ensure monochromatic radiation.

Modeling of the zirconium octadecylphosphonate structure was performed using SYBYL (Tripos Associates) Molecular Modeling program. In SYBYL, the CRYSIN mode was used to import crystallographic coordinates[18] for α-$Zr(HPO_4)_2 \cdot H_2O$. An octadecyl hydrocarbon chain, using the BUILD mode, was grafted onto the structure to simulate the zirconium octadecylphosphonate structure.

X-ray photoelectron spectra were obtained using a Perkin-Elmer (Norwalk, CT) PHI 5000 Series spectrometer. All spectra were taken using the Mg Kα line source at 1253.8 eV. The spectrometer has a resolution of 2.0 eV with anode voltage and power settings of 15 kV and 300 W, respectively.

Typical operating pressure was 5 x 10^{-8} atm Survey scans were performed at a 45° take-off angle with a pass energy of 89 45 eV Multiplex scans (140 scans) were run over a 20 to 40 eV range with a pass energy of 17 90 eV

Transmission electron diffraction experiments were preformed on a JEOL (Peabody MA) JEM 400CX electron microscope A 200 kV accelerating voltage was used with the electron beam normal to the LB basal plane

Results and Discussion

Octadecylphosphonic Acid Monolayers

Octadecylphosphonic acid spreads at the air/water interface [48] The surface pressure vs area (π-A) isotherm (Figure 2-3 curve A) of octadecylphosphonic acid on a pure water subphase using a single barrier trough yields an extrapolated cross-sectional area of 24 Å^2/molecule with a collapse pressure occurring at a surface pressure of 60 mN/m A Creep test[52] is

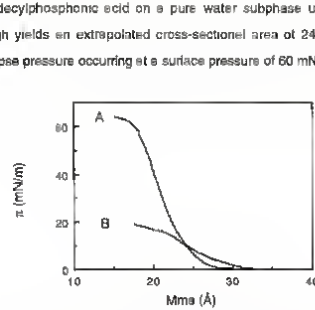

Figure 2-3 Isotherms of octadecylphosphonic acid on a pure water subphase (curve A) and on a Zr^{4+} subphase (curve B) at 25° C Due to the rigid nature of the film in curve B, an accurate pressure measurement is not possible

performed on the octadecylphosphonic acid monolayer in order to measure the stability of the floating monolayer film (Figure 2.4). In this experiment the octadecylphosphonic acid molecules are compressed to a specific pressure, namely 20 mN/m, and held at that pressure while the change in trough area is monitored as a function of time. The octadecylphosphonic acid film possesses a creep of 0.5mm/min (change in area is 47 mm^2/min) which indicates that some of the film is being lost on the trough, possibly due to dissolution of the molecules into the subphase. Upon addition of Zr^{4+} ions to the water subphase, the octadecylphosphonic acid Langmuir monolayer becomes extremely rigid.[46,47] The π-A isotherm of octadecylphosphonic acid on a Zr^{4+} subphase is curve B in Figure 2-3. As the film is compressed, the pressure begins to increase at 31 $Å^2$, but the actual collapse pressure is not obtained. The Wilhelmy plate is pushed from the vertical during compression leading to an inaccurate measure of surface pressure. This suggests that the Zr^{4+} ions bind and crosslink the phosphonic acid groups at the air/water interface creating a rigid film.

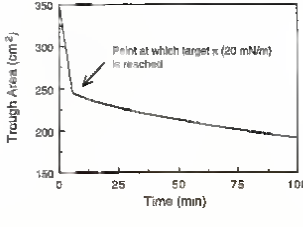

Figure 2-4 Creep test for octadecylphosphonic acid on a pure water subphase at 25^0 C

Brewster Angle Microscopy

Brewster angle microscopy[53,54] (BAM) is based on the principle of optical reflection at an interface. When p polarized light is focused on the air/water interface at the Brewster angle (α) for water, which is defined as

$$\tan(\alpha) = n_2/n_1 \qquad (2\text{-}1)$$

where n_1 and n_2 are the refractive indices of the air and water, respectively, no light is reflected. When a monolayer is then formed at the air/water interface and possesses a refractive index different from water, light is then reflected from the monolayer. The reflected light can be monitored by a CCD camera producing images of the monolayer at the air/water interface. BAM images confirm the rigid nature of the octadecylphosphonic acid film formed on a Zr^{4+} subphase. Figure 2.5 shows BAM data for octadecylphosphonic acid compressed on a pure water subphase using a dual barrier trough. The images are obtained from three different pressures during compression that are indicated on the π-A isotherm. The light grey areas (reflected light) represent the octadecylphosphonic acid film, whereas the dark areas (no reflection) represent the water subphase. The film is "fluid" upon spreading and melds together as it is compressed to form a continuous film. Figure 2-6 shows BAM data for octadecylphosphonic acid compressed on a Zr^{4+} subphase. The addition of Zr^{4+} ions causes aggregation of the amphiphiles immediately upon spreading of the molecules. The domains that are formed upon spreading maintain their shape throughout compression and decompression of the monolayer. The domains that are formed during spreading of the monolayer at

Figure 2-5 Brewster angle microscopy of octadecylphosphonic acid spread on a pure water subphase. The images correspond to the three regions marked on the isotherm

π (mN/m)
Mn² Å

Figure 2.6 Brewster angle microscopy of octadecylphosphonic acid compressed on a 5mM Zr^{4+} ion subphase. The images correspond to the three regions marked on the isotherm

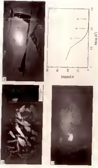

the air/water interface are believed to be due to the Zr^{4+} ions cross-linking the phosphonic acid groups at the air/water interface creating a rigid film. Because of the rigid nature of this film, conventional vertical LB deposition was not successful. Therefore, we have developed a new stepwise deposition procedure[46,47] that takes advantage of the strong zirconium-phosphonate interaction and combines the LB technique with "inorganic" self assembly methods to prepare monolayer and multilayer films of zirconium octadecylphosphonate.

Deposition Procedure

The procedure developed for depositing zirconium phosphonate films is outlined in Figure 2-7. The method combines LB and SA deposition techniques. The first step is to create an LB template of octadecylphosphonic acid suitable for binding Zr^{4+} ions. This is achieved by transferring a single LB layer of octadecylphosphonic acid from a pure water subphase onto an OTS-covered substrate. OTS is used to modify the SiO_2 surface to produce a hydrophobic substrate. This substrate is dipped down through the monolayer film into a vial sitting in the subphase. The film is transferred to the OTS-covered substrate by a hydrophobic interaction, which produces a single-layered film with phosphonic acid sites extended from the substrate. The Langmuir monolayer is then decompressed, and the vial containing the octadecylphosphonic acid-coated slide, now immersed in the subphase, is removed from the trough. The second step is to "self-assemble" the Zr^{4+} ions at the organic template by adding enough $ZrOCl_2$ to the vial to produce a 5mM zirconium solution. In this step, the phosphonic acid template binds the Zr^{4+} ions from solution. After 30 minutes, the substrate with the zirconated template

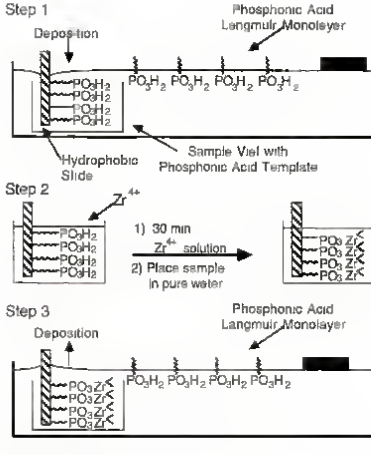

Figure 2-7 Deposition procedure for the preperation of zirconium octadecylphosphonate films

layer is removed from the Zr^{4+} solution and placed into another vial containing pure water. When the substrate is removed from the Zr^{4+} solution it is completely wetted indicating that a hydrophilic surface is produced which suggests that the phosphonic acid-Zr^{4+} sites are extended from the surface. The final step is to bind the capping layer to complete the bilayer assembly. The film-containing substrate in pure water is placed back into the LB trough, where a new octadecylphosphonic acid film is compressed over the vial, and is then transferred to the substrate creating a Y-type zirconium octadecylphosphonate bilayer. After the deposition of the capping layer the sample is dry indicating that a hydrophobic surface is produced and that all of the phosphonic acid-Zr^{4+} sites have been capped by a second octadecylphosphonic acid layer. Contact angle measurements on bilayer and multilayer films result in an advancing contact angle of $112^{o} \pm 1^{o}$. This demonstrates that the outermost surface of the substrate consists of methyl groups. Multilayers are prepared by repeating the deposition procedure.

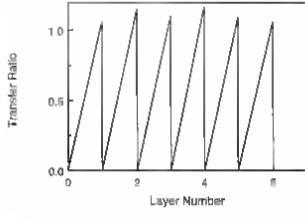

Figure 2.6 Transfer ratios of octadecylphosphonic acid

Octadecylphosphonic acid was transferred at a constant surface pressure of 20mN/m. The transfer ratios of the tail-to-tail (odd layer number) and head-to-head (even layer number) depositions (Figure 2.8) range between 1.1 and 1.2 because they have not been corrected for the creep of the film.

Infrared Spectroscopy

IR spectroscopy can be used to monitor and characterize transferred films.[13,55,56] The zirconium octadecylphosphonate films were transferred onto OTS-coated Si ATR crystals in order to obtain IR spectra. Figure 2-9 compares the FTIR spectrum, from 2500 cm^{-1} to 3200 cm^{-1}, of the deposited LB monolayer template after binding of Zr^{4+} ions (after step 2 in Figure 2-7) to the spectrum of a zirconium phosphonate bilayer (after step 3 in Figure 2-7). Also shown in Figure 2-9 is the spectrum of a multilayer film (3 bilayers) formed by repeating the deposition process. In each spectrum three bands are resolved.[13,55] The asymmetric CH_3 stretch ($\nu_a(CH_3)$) at 2960 cm^{-1}, the asymmetric CH_2 stretch ($\nu_a(CH_2)$) at 2918 cm^{-1}, and the symmetric CH_2 stretch ($\nu_s(CH_2)$) at 2852 cm^{-1}. The $\nu_s(CH_2)$ band has been shown to be useful in understanding the order and packing of the aliphatic chains in monolayers.[55] The band frequency is indicative of the conformational order[13,55] and ranges from 2918 cm^{-1} in an all-trans conformation to 2924 cm^{-1} in a "liquid-like" alkane that contains a large percentage of gauche bonds. The full width at half maximum (fwhm) is a measure of the orientational order.[13,56] For example, the fwhm of an OTS monolayer is 17 cm^{-1} whereas a randomly oriented film[46,47] can result in a fwhm of greater than 35 cm^{-1}. For a bulk sample of octadecylphosphonic acid the $\nu_s(CH_2)$ band frequency ranges from 2918 cm^{-1} with a fwhm of 21 cm^{-1} in the crystalline solid to 2924 cm^{-1} with a fwhm of 35 cm^{-1} in solution.[45,47] In all

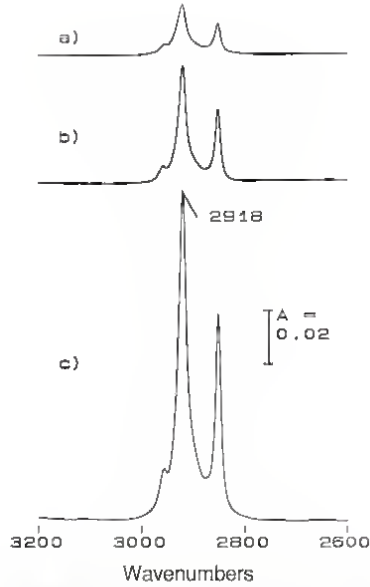

Figure 2-9 Infrared spectra of zirconium octadecylphosphonate films: zirconated LB template (top), zirconium phosphonate bilayer (middle), zirconium phosphonate multilayer film (bottom)

three spectra presented in Figure 2-9 the frequency of the $\nu_s(CH_2)$ band is 2916 cm^{-1} and the fwhm is 20 cm^{-1} indicating that the aliphatic chains are close packed and possess an all trans conformation Progressing from template layer to bilayer, the intensities of the C-H bands double, but the position and appearance of the bands remain unchanged indicating that the structure of the film does not change during the deposition process Figure 2 10 plots the intensity of the $\nu_s(CH_2)$ band versus the number of bilayers for multilayer films The linear increase in intensity suggests that the same amount of material is deposited after each complete deposition and is consistent with a layer-by-layer deposition as suggested by the transfer ratio data

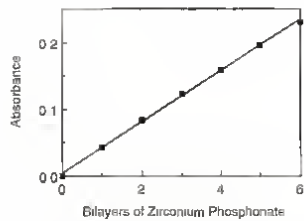

Figure 2 10 Infrared absorbance of the $\nu_s(CH_2)$ stretch versus the number of zirconium octadecylphosphonate bilayers transferred to a Si ATR crystal

X-ray Photoelectron Spectroscopy

X ray photoelectron spectroscopy (XPS) is useful to analyze LB films and determine the chemical species present.[57] XPS is an analytical technique which can provide chemical and physical data on the first few nanometers of a

sample surface. In the XPS a sample is bombarded with monoenergetic X-rays. The X-rays interacts with the atoms present in the sample causing core electrons to be emitted (Figure 2-11). These core electrons are emitted from specific binding energies which can be used to distinguish atoms present in the sample. The energetics of the experiment can be described as:

$$hv = BE + KE \qquad (2\text{-}2)$$

where hv is the photon energy, BE is the binding energy of the electron which is ejected and KE is the kinetic energy of the electron.

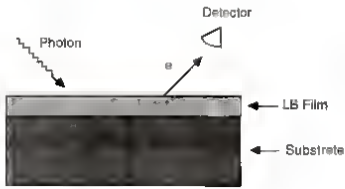

Figure 2-11. Schematic of the XPS experiment.

XPS analysis shows that C, Si (substrate), O, P, and Zr are the only elements present in the deposited zirconium octadecylphosphonate films. Figure 2-12 shows XPS multiplex spectra of the Zr 3d and P 2p peaks for a template film capped with zirconium (top), a zirconium phosphonate bilayer (middle), and three zirconium phosphonate bilayers all on OTS-covered silicon (bottom). Using the appropriate instrument and atomic sensitivity factors[58,59]

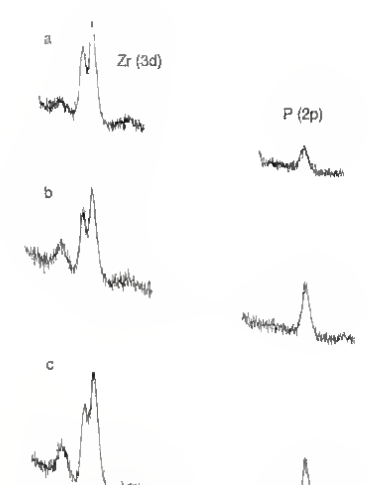

Figure 2-12. XPS multiplex spectra of zirconium octadecylphosphonate films zirconated LB template layer (top) zirconium phosphonate bilayer (middle) zirconium phosphonate multilayer film (bottom)

relative observed intensities attained from the integrated signals are accurate to within 10% [57]

A model was derived from the attenuation equation[60] in order to predict the relative elemental intensities of Zr and P in the sample. The distance of each element from the outermost surface is calculated from known interatomic distances [12,61]. The result is a model matrix in which there are discrete layers of elements each separated by some distance, d, from the outermost surface. Each atom, A, in the sample will contribute a term:

$$I_A = I_A^{\infty} \exp(-d_m/(\lambda_m \sin\Theta)) \qquad (2.3)$$

to the spectrum[57] in which I_A^{∞} is the peak area normalization or sensitivity factor [58], d_m is the overlayer thickness of material m, in this case an LB layer, λ_m is the inelastic mean free path of the photoelectron through material m, and Θ is the take-off angle with respect to the surface parallel. The above term gives a calculated relative intensity, I_A, of element A when multiplied by a stoichiometric factor and summed over each A containing layer in the matrix. The inelastic mean free path λ_m is dependent upon the kinetic energy of the photoelectron and upon the material through which the escaping photoelectron travels. For organic layers, literature values of λ_m vary by about an order of magnitude [28,60,62,63]. According to the first spectrum in Figure 2-12, after zirconium ions bind to the octadecylphosphonic acid template layer, the observed relative intensities for Zr and P are 53% and 47%, respectively. The observed relative intensity suggest that the Zr atoms are in greater abundance than the P atoms. In obtaining relative peak intensities, the attenuation length of the electrons and the depth of each species present in the film must be taken into consideration. For Zr and P, the attenuation lengths are almost identical [60]

therefore, the depth of each species from the surface will contribute to the differences in observed peak intensities for Zr and P. An idealized schematic shown in Figure 2-13 depicts the different distances that the electrons must travel to "escape" from the film. We have calculated using the attenuation equation that a Zr:P ratio of 1:1 for this type of monolayer will produce a relative intensity of 51 % and 49 % (Table 2-1) for the Zr species and the P species, respectively.

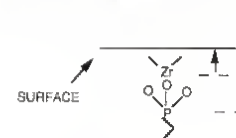

Figure 2-13. Representation of the distance electrons must travel in the XPS analysis of the zirconated LB template.

The calculated relative intensities and the observed relative intensities are in excellent agreement. The 1:1 Zr:P relative ratio for the zirconated template layer indicates that the molecules in the octadecylphosphonic acid film are spaced to allow one zirconium ion per phosphonate group, and that the film is close packed so that the molecules cannot rearrange to bind two phosphonates to a single zirconium ion. After capping the template with a second octadecylphosphonic acid LB layer (middle spectrum of Figure 2-12), the P:Zr ratio is 2:1 (Table 2-1) which is consistent with the stoichiometry observed in the bulk layered zirconium phosphonates.[33-35] Finally, the lower spectrum in Figure 2-12 shows a 2:1 P:Zr ratio (Table 2-1) in the film containing

three bilayers indicating that the chemical content of the film remains the same as multilayered films are deposited

Table 2-1 XPS analysis of zirconium octadecylphosphonate films.

Film Type	Calculated Relative Intensities		Observed Relative Intensities[a]	
	Zr 3d	P 2p	Zr 3d	P 2p
Zirconated Template Layer	51%	49%	53%	47%
Zirconium Phosphonate Bilayer	32%	68%	33%	67%
Zirconium Phosphonate Multilayer	32%	68%	33%	67%

a Relative intensities are determined from atomic and instrument sensitivity factors [58,59]

Ellipsometry and X-ray Diffraction

Reflection ellipsometry (2-14) is useful in determining the thickness of deposited films and monitoring a layer by layer deposition [25,67] In this experiment linearly polarized light is reflected from a surface which causes a change in the phase and amplitude of the parallel and perpendicular components of the light

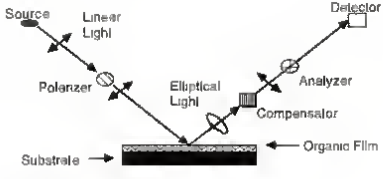

Figure 2-14 Ellipsometry experiment.

The changes in the phase and the amplitude are determined by two parameters Ψ and Δ which are defined as [12,87]

$$\Psi = (180 - [A2 - A1])/2 \qquad (2\text{-}4)$$

$$\Delta = 360 - [P1 + P2] \qquad (2\text{-}5)$$

where A1 and A2 are the two analyzer settings and P1 and P2 are the two polarizer settings. From Ψ and Δ the thickness and refractive index can be solved simultaneously. Ellipsometric results (Figure 2-15) show a linear increase in film thickness with each successive bilayer. Thicknesses are obtained using an index of refraction of 3.54 for the Si substrates and 1.49 for the zirconium alkylphosphonate films.

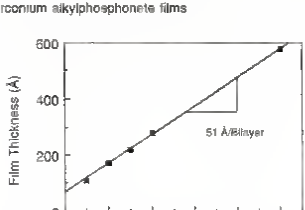

Figure 2-15. Thickness of the zirconium octadecylphosphonate films versus the number of bilayers. The solid line is a best fit regression line.

From the slope of the regression line a thickness of 51 Å ± 5 Å per bilayer is calculated. The fact that the regression line does not pass through the

origin s expected The template films are transferred onto an OTS covered silicon wafer with an unknown oxide thickness The combination of the oxide layer and OTS produces an initial film thickness which is constant throughout the experiment

While ellipsometric results are consistent with layer-by-layer deposition, it should be remembered that ellipsometry yields an average film thickness [57] but does not prove that the films indeed possess a layered structure Ellipsometry should be used in conjunction with other experimental data and here the ellipsometric results are confirmed by low angle X-ray diffraction Figure 2 16 shows X-ray diffraction from twelve bilayers of zirconium octadecylphosphonate on a silicon substrate Four orders of the (00*l*) reflection, including the (001) can be identified

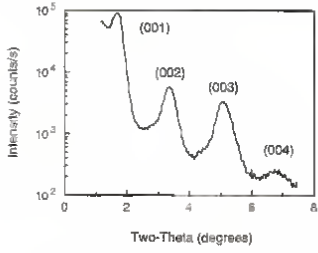

Figure 2 16 Low-angle x-ray diffraction from twelve bilayers of zirconium octadecylphosphonate

Using the Bragg equation which is defined as

$$n\lambda = 2d(\sin\theta) \qquad (2\text{-}6)$$

where n is the order of reflection λ is the wavelength of the X-ray d is the distance between planes (d spacing) and θ is the angle of the incoming X-ray with respect to the surface parallel the distance between Zr^{4+} planes can be determined The data correspond to a d-spacing of 52 Å for the zirconium octadecylphosphonate films in excellent agreement with the ellipsometric data More importantly however diffraction proves the layered nature of the films.

Structure of Monolayer and Multilayer Films

Steps 1 and 2 of the deposition method outlined in Figure 2-7 represent an example of "inorganic self-assembly" at an organic template The LB method is first used to arrange the octadecylphosphonic acid molecules into an organized assembly that is similar to the packing the alkylphosphonates assume in the three dimensional solid state structure From structural data[33] of solid α-$Zr(HPO_4)_2\,H_2O$ the intermolecular distance between phosphonic acid molecules corresponds to a mean molecular area of 24 7 $Å^2$/molecule in the zirconium ion plane while the mean molecular area of the octadecylphosphonic acid LB film is 24 $Å^2$/molecule [46 47] This arrangement provides a surface that allows the binding from solution of one zirconium ion per phosphonate group at the surface as confirmed by the XPS data in Figure 2-12 and prohibits the phosphonate molecules from folding over to bind more than one phosphonate group per zirconium ion

Addition of the capping phosphonic acid layer completes the metal phosphonate bilayer The bilayer films as well as the multilayer films have structures similar to those observed for solid zirconium phosphonates XPS

shows that the films have the $Zr(O_3PR)_2$ stoichiometry and X ray diffraction proves that the films possess a layered structure The complete analysis is in accord with a structure that consists of layers of zirconium ions bonded by phosphonate groups that extend above and below the plane forming a layer of close packed alkyl chains We attempted to model the zirconium octadecylphosphonate bilayers with the SYBYL molecular modeling program. Using crystallographic coordinates for α-$Zr(HPO_4)_2 \cdot H_2O$[33] to model Zr-O_3P binding a bilayer was generated by grafting on a $(CH_2)_{17}CH_3$ chain in place of the phosphate OH In the generated structure the all-trans hydrocarbon chain lies at a tilt angle of 31.3° with respect to the zirconium ion plane (Figure 2 17) which is a consequence of the phosphonate P-C bond orienting nearly perpendicular to the plane of metal ions just as the P-OH bond is oriented in the α-$Zr(HPO_4)_2 \cdot H_2O$ structure[33] The resulting Zr-Zr interplane spacing is 42 8 Å It the alkyl chains are rotated such that the chain axes are oriented perpendicular to the zirconium ion plane the maximum expected interlayer spacing is 53 7 Å The experimentally determined interlayer spacing of 52 Å for the zirconium octadecylphosphonate films lies within the 42 8 – 53 7 Å range determined from modelling The 52 Å spacing however requires the phosphonate alkyl chain to orient nearly perpendicular to the plane of metal ions which would force the Zr O_3P binding to differ from that observed for α–$Zr(HPO_4)_2 \cdot H_2O$

In the α–$Zr(HPO_4)_2 \cdot H_2O$ (Figure 2-2) the phosphonate group sits above an equilateral triangle of Zr^{4+} ions with phosphate oxygens binding three different metal ions in the triangle[33] The phosphate groups are bridged by zirconium ions such that oxygen atoms that form the octahedral coordination come from six different phosphates three in the plane above and three in the plane below the zirconium ion plane In the zirconium octadecylphosphonate

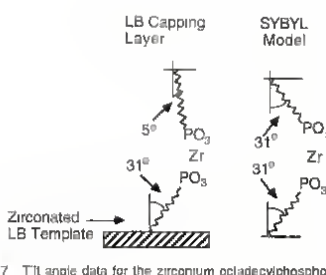

Figure 2.17 Tilt angle data for the zirconium octadecylphosphonate SYBYL model and LB bilayer

bilayers, in order for the phosphonate alkyl chain to orient perpendicular to the metal ion plane the tetrahedral RPO_3 group must be tilted such that the three phosphonate oxygens no longer have equivalent orientations relative to the plane of zirconium ions. Such an arrangement has been observed in some γ phase layered zirconium phosphates [68 70] In the series γ-$Zr(HPO_4)(n\text{-}C_nH_{2n+1}PO_4)$ yH_2O [68 70] the interlayer spacing increases with the alkyl chain length, and the slope of this increase is consistent with the phosphate groups orienting with their alkyl chain axes perpendicular to the zirconium ion plane Because only every other phosphate is alkylated in the γ-phase materials the alkyl chains fold over in the longer chain derivatives in order to maximize the van der Waals contact between the hydrocarbon chains [68-70] Upon intercalation with n-alcohols however the alkyl groups reorient themselves perpendicular to the zirconium plane and fill the voids in the organic layer [68 70] Yamanaka and coworkers have prepared a number of intercalated derivatives including the octadecyl analog[70] where X ray diffraction shows the interlayer

spacing to be 52 Å which is exactly the thickness observed for the zirconium octadecylphosphonate films

Polarized ATR-FTIR[71,72] was used to determine the molecular axis tilt for the phosphonic acid template layer and the capping phosphonic acid layer. The zirconated template layer was determined to have a molecular axis tilt of 31° from the normal with respect to the surface (Figure 2.17) which is in excellent agreement with the SYBYL model. However, the capping octadecyl phosphonic acid layer possesses a molecular axis tilt of 5° from the normal with respect to the surface. The combination of the two tilt angles leads to a thickness of approximately 49 Å for the bilayer. The tilt angle data indicates that the zirconium phosphonate organization resulting from the layer-by-layer deposition developed here is different from the α-phase and the γ phase materials. The formation of the octadecylphosphonic acid template layer resembles the α-phase materials and is held in place by the assembly of the Zr^{4+} ions. However, the assembly of the capping octadecylphosphonic acid layer by the Langmuir-Blodgett technique forces an orientation on the capping layer that resembles the γ-phase materials by aligning the alkyl chains of the molecules perpendicular to the air/water interface. This perpendicular arrangement of the floating octadecylphosphonic acid monolayer is preserved by the strong zirconium binding which occurs upon transfer of the capping layer. The difference in tilt angles suggest that the LB technique can control and direct the orientation of assembled films.

Transmission electron diffraction (TED) was also performed on a ten bilayer sample in an attempt to determine the in-plane Zr-O_3P structure. We observed a hexagonal diffraction pattern that corresponds to a d-spacing of 4.26 Å ± 0.15 Å. This d-spacing is similar to d-spacings observed in stearate LB films.[73-75] It is likely that the diffraction pattern observed arises from the

crystalline alkyl chains of the phosphonate groups and does not arise from Zr^{4+} ion plane

Solid zirconium phosphonates are highly insoluble in both water and organic solvents and the zirconium phosphonate films described here are similarly insoluble Figure 2.18 compares IR spectra of a ten-bilayer film before and after soaking in chloroform for 60 and 120 minutes After 60 minutes the $\nu_a(CH_2)$ is still at 2918 cm^{-1} with fwhm of 20 cm^{-1}, but approximately 20% of the film has been lost After this spectrum was taken the film was placed back into chloroform for another 60 minutes and the spectrum recorded again That the frequency and shape of the IR band remain constant after the first soaking in chloroform indicates that the remaining film is still close packed and does not rearrange We hypothesize that the original soaking washes away defect areas of the film and that what remains is the insoluble zirconium phosphonate

The approach of using an organic monolayer to organize the inorganic monolayer is similar to the concept of using Langmuir monolayers to influence nucleation and crystal growth of inorganic solids from an LB subphase [15-20,76,77] Heywood and coworkers[15-19] have shown that crystals of the inorganic salts $CaCO_3$[17-19] and $BaSO_4$[15,16] can be grown from saturated solutions at Langmuir monolayers of surfactant molecules and that the choice of surfactant can influence the orientation and growth of specific crystal faces or even regulate the selectivity of crystal polymorphs Studies by Landau *et al* [76,77] have demonstrated similar control on the growth of glycine crystals at Langmuir monolayers of resolved amino acids In these studies the Langmuir monolayer serves as a template for nucleation, where the intermolecular spacing of the template as well as the stereochemical and electrostatic nature of the interface can be controlled by choice of surfactant molecule The work we present here is similar in that the organic layer is first organized in order to

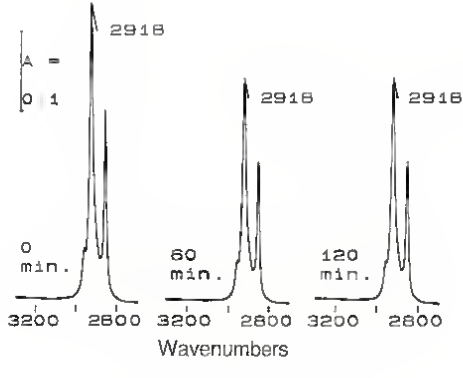

Figure 2-18 Infrared spectra of a ten-bilayer zirconium octadecylphosphonate film (left) before and after soaking in chloroform for 60 min (middle) and 120 min (right)

control the molecular spacing of the inorganic material, while in contrast we restrict the growth of the inorganic lattice to a single layer. In addition, the template layer used here is not a floating monolayer, rather the template is placed onto a solid support.

The stability of these films in both aqueous and organic solvents suggests a that zirconium phosphonate films could be useful in preparing materials that require organized assemblies of organic molecules analogous to other LB[78] and SA[40-42,79] work on preparing films with second order non-linear optical properties. While the LB method is ideally suited to orienting organic molecules, thin films are generally metastable and the desired physical effects decay with time. The films described here are modeled after a known layered solid-state structure, and the thermodynamic stability of the zirconium phosphonate structure greatly enhances the durability of these films suggesting that the preparation procedure described herein should be considered for preparing materials that require organized organic assemblies. Other groups[40-42] have taken advantage of strong zirconium phosphonate binding in forming *self-assembling* multilayer films for nonlinear optical[40-42] applications. A feature of the LB deposition process, however, is that a close packed phosphonic acid template is assured, generating the optimum density of sites for binding zirconium ions. This should lead to a higher density of active organic molecules in the mixed organic/inorganic assembly as well as a higher degree of orientation.

Summary

We have demonstrated that an organized organic monolayer can be used as a template for assembling an extended-lattice inorganic monolayer. A

stepwise procedure has been developed for forming monolayer and multilayer films of zirconium octadecylphosphonate that uses an LB film of octadecylphosphonic acid to provide an organized surface for binding Zr^{4+} ions from solution. The zirconium phosphonate structure is completed by capping the surface with a second octadecylphosphonic acid LB film. Analysis of bilayer and multilayer films is consistent with forming layers on the surface whose structure is different than that of solid layered zirconium phosphonates. As will be shown in the next chapter, the approach of using organized monolayers for preparing inorganic monolayer films should be applicable to other layered organic/inorganic systems including systems that have been used to model two-dimensional conductors and magnets.

CHAPTER 3
THE ROLE OF THE TEMPLATE LAYER IN ORGANIZING SELF ASSEMBLED FILMS ZIRCONIUM PHOSPHONATE MONOLAYERS AND MULTILAYERS AT A LANGMUIR-BLODGETT TEMPLATE

Introduction

The promise of directing the properties of systems by controlling the architecture orientation and density of molecules within organized assemblies is currently an important driving force in many aspects of chemical research In developing organized thin films the Langmuir Blodgett[10-12] (LB) technique along with various procedures for the "self-assembly" (SA) of organic molecules at surfaces[12 14 21 22] are examples of methods that produce functional assemblies through the purposeful manipulation of molecules Applications that make use of thin films often require multilayers and while depositing multilayer LB films is straightforward there are only a few self assembly routes to multilayer films [2,23-28 79 80] The potential advantages of self-assembled multilayers include less complicated processing and the structural stability afforded by covalent linkages between the layers A remaining question [43 81] however is to what degree can orientational and position order be achieved among molecules in self-assembled multilayer structures

The first report of multilayer films prepared by organic self assembly was published by Sagiv and coworkers[23] and was discussed in chapter 2 Briefly molecules possessing a terminal olefin are adsorbed onto an oxide surface The olefin surface is then chemically converted to produce a surface of hydroxyl functionalities (Figure 3 1) The OH terminated surface can adsorb another

monolayer layer and by repeating the process multilayer films can be constructed. Several other groups[79-80] have followed similar methodologies in order to prepare multilayer films.

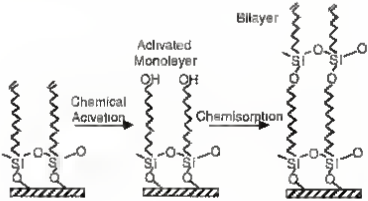

Figure 3:1 The first report of multilayer films prepared by organic self assembly

Procedures have also been developed where self assembled organic layers are linked by transition metal ions.[2,24-29] Mallouk and coworkers[2,24-27,29] demonstrated a method for one-layer-at-a-time depositions of α,ω-diphosphonic acids that takes advantage of the strong affinity of phosphonate (or phosphate) groups for the Zr^{4+} ion. In this procedure (Figure 3:2) a molecule bearing the phosphonic acid functionality is adsorbed to a surface and layers are built-up by alternately adsorbing Zr^{4+} ions and α,ω-diphosphonic acid molecules from solution. Thin films formed in this way have been used as the dielectric in metal-insulator-semiconductor and metal-insulator-metal devices.[29] Katz and coworkers[48-44] have adapted this procedure to prepare films containing oriented assemblies of a wide variety of functionalized molecules. Among the properties demonstrated in such films are interlayer electron transfer[44] and second harmonic generation.[41]

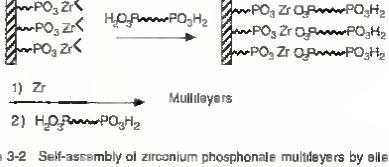

Figure 3-2 Self-assembly of zirconium phosphonate multilayers by alternately adsorbing Zr^{4+} ions and α,ω-diphosphonic acids from solution

Several methods have been described for prepering the initial phosphonate derivatized surface [24 25 40 41]. The original work adsorbed 3-(hydroxydimethylsilyl)propyl phosphonic acid to oxide surfaces [24 25] and the disulfide $[S(CH_2)_4PO_3H_2]_2$ to Au electrodes [25]. Another approach includes reacting $POCl_3$ with the polymer derived from 3-(aminopropyl)-trimethoxysilane [40 41]. Efforts to increase the organization of the surface layer have taken advantage of the "self assembling" quality of longer alkyl chain derivatives. Triethoxysilylnonadecylacetate[43] and triethoxysilyloctadecyl-bromide[45] have been self assembled to oxide surfaces and subsequently transformed to phosphonic acid derivatives on the surface. Katz et al [43] have also directly deposited 19-thiononadecylphosphonic acid onto Au surfaces for the build up of zirconium phosphonate multilayers.

In the previous chapter the use of LB methods to prepare single layer analogs of the solid-state zirconium phosphonates was described. We detailed a procedure for zirconating an LB monolayer of octadecylphosphonic acid. The LB layer provides an organized array of phosphonate sites at the surface that we have shown is close packed and coordinates one zirconium ion per phosphonate group [47]. We have found that this LB method produces a more organized phosphonate derivatized surface than does any of the SA methods

that we have investigated. In this present chapter we describe how this zirconated LB layer can be used as a "template" for self-assembling organophosphonates. Starting with a well characterized and ordered "template" layer we can quantify subsequent self assembly steps and learn how the order and packing density of the template layer extends to the built-up layers. To this end we have studied the self-assembly of a monolayer of octadecylphosphonic acid at the LB template as well as the build-up of multilayer films using 1,10-decanediyldiphosphonic acid. In analogy to the original procedure described by Mallouk[24,25] We have also investigated use of the LB template for depositing a rigid molecule, quaterthiophenediphosphonic acid (QDP) (Figure 3-3) which was developed by Howard E. Katz and coworkers[40] for the purpose of building-up electron-rich multilayered thin films one layer at a time.

Figure 3-3 Quaterthiophenediphosphonic acid (QDP)

We monitor the deposition processes by FTIR, contact angle, XPS, ellipsometry, UV-vis, and X-ray diffraction. We show that a high degree of orientational order can be achieved in self-assembled organophosphonate layers, and that the organization of functional sites in the initial template layer is an important factor. For example, the rigid QDP molecule assembles with sufficient orientational order at the zirconated LB template that Bragg diffraction is observed from 10 layers self assembled onto a planer surface.

Experimental Section

Materials

Octadecylphosphonic acid ($C_{18}H_{39}O_3P$) and 1,10- decanediyl diphosphonic acid ($C_{10}H_{24}O_6P_2$) (DDPA) were prepared in our lab by Margaret Showalter[45] from octadecylbromide and 1,10-dibromodecane, respectively by the Michaelis-Arbuzov[49] reaction, followed by acid hydrolysis. Both acids were recrystallized twice from ethanol. Quaterthiophenedi-phosphonic acid (QDP) was provided by Dr. Howard Katz.[40] Zirconyl chloride, 98% was used as purchased from Aldrich (Milwaukee, WI).

Substrate Preparation

Single crystal (100) silicon wafers, purchased from Semiconductor Processing Company (Boston, MA), were used as deposition substrates. Silicon attenuated-total reflectance (ATR) crystals, (50mm x 10mm x 3mm) purchased from Wilmad Glass (Buena, NJ) were used as substrates for all infrared experiments. Silicon ATR crystals were parallelograms, with a 45° angle of incidence with respect to the parallel faces. The silicon substrates were cleaned using the RCA cleaning procedure[50] then dried under N_2. All octadecyltrichlorosilane (OTS) coated surfaces were prepared by placing the cleaned substrates in a 2% solution of OTS in hexadecane for 30 minutes. Substrates were then rinsed with chloroform to remove any excess hexadecane then dried under flowing N_2. Glass microscope slides (76.4mm x 25.4mm x 1mm) purchased from Fisher Scientific (Orlando, FL) used in all UV/vis experiments were cleaned as the silicon substrates.

Instrumentation

The Langmuir Blodgett experiments were performed using KSV Instruments (Stratford CT) PFTE (teflon) coated LB troughs with hydrophobic barriers. A Barnstead NANOpure purification system produced water with a resistivity of 18 MΩ–cm for all experiments. Depositions were carried out using a KSV 3000 system and in all cases films were compressed linearly at a rate of 5mN/m/min at room temperature. For the depositions, a target pressure of 20mN/m was maintained with deposition speeds of 10mm/min for both the up and down strokes were used.

Infrared spectra were recorded with a Mattson Instruments (Madison WI) Research Series-1 Fourier transform infrared (FTIR) spectrometer using a narrow band mercury cadmium telluride detector. A Harrick (Ossining, NY) TMP stage was used for the ATR experiments. Polarized FTIR-ATR spectra were taken with s- and p-polarized light. All spectra consist of 1000 scans at 2.0 cm^{-1} resolution and were ratioed to the OTS-covered substrates or the appropriate s- or p-polarized background.

Advancing contact angle measurements were measured with a Rame-Hart (Mountain Lakes NJ) NRL Contact Angle Goniometer Model 100-00. A 250 mL syringe was used to dispense a fixed volume advancing water drop to the surface.

Ellipsometry measurements were obtained with a Rudolph Instruments Series 431A Universal Ellipsometer (Fairfield, NJ). A He-Ne laser (632.8 nm) was used as the light source. The angle of incidence was set at 70° for all experiments. The parameters Ψ and Δ were estimated from the polarizer and analyzer settings. The refractive index and thickness of the films were

calculated using an in house computer program. Silicon was the only substrate used for this experiment.

X-ray photoelectron spectra were obtained using a Perkin-Elmer (Norwalk, CT) PHI 5000 Series spectrometer. All spectra were taken using the Mg Kα line source at 1253.6 eV. The spectrometer has a typical resolution of 2.0 eV, with anode voltage and power settings of 16 kV and 300 W, respectively. Typical operating pressure was 5×10^{-9} atm. Survey scans were performed at a 45° take-off angle with a pass energy of 89.45 eV. Multiplex scans, 140 scans at each peak, were run over a 20 to 40 eV range with a pass energy of 37.75 eV. In all cases, the observed relative intensities are determined from experimental peak areas normalized with atomic and instrument sensitivity factors.[58,59]

UV-vis spectra were obtained with a Hewlett-Packard 8452A diode array spectrometer. The incident beam was aligned perpendicular to the substrate.

Low-angle X-ray diffraction was performed with a Rigaku 18 kW rotating anode diffractometer. The X-ray source was the Cu Kα line, $\lambda = 1.54$ Å, which was first passed through a graphite monochromeler.

Results and Discussion

The Template Layer

The preparation and characterization of the zirconated LB template layer (Figure 3-4) that is used in the SA experiments reported here is described in detail in the previous chapter. Briefly, an octadecylphosphonic acid Langmuir monolayer is transferred tail-to-tail to an OTS-covered substrate by dipping the substrate down through the air/water interface and into a vial which is immersed

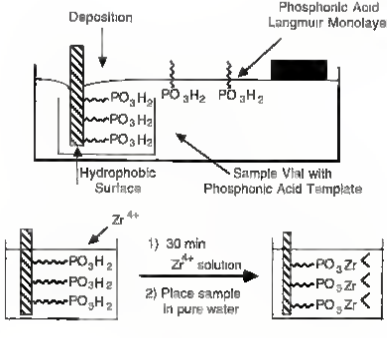

Figure 3-4 Deposition procedure for the preparation of the zirconated LB template layer

in the trough. The vial containing the phosphonic acid-coated substrate is then removed from the trough, and $ZrOCl_2$ is added to the vial. The binding of zirconium ions to the LB template layer is complete within 30 min, and the substrate is rinsed with water before reaction with solutions of the organophosphonates. According to XPS analysis (discussed in chapter 2) the Zr:P ratio (Table 3-1) in the zirconated template film is 1:1, and reveals that each phosphonic acid in the LB film binds a Zr^{4+} ion.

Table 3.1. XPS Multiplex Data for Zirconium Phosphonate Layers

Film Type	Elements	Peak/Area[a]	Obs. Rel. Int.[b]
Zirconated LB Template Layer	Zr	Zr 3d/1306	53.0
	P	P 2p/215	47.0
Self Assembled Octadecylphosphonic Acid Bilayer	Zr	Zr 3d/3795	31.0
	P	P 2p/1589	69.0
Langmuir-Blodgett Octadecylphosphonic Acid Bilayer	Zr	Zr 3d/919	33.1
	P	P 2p/345	66.9

a. The units for Area are (counts eV)/sec. b. Relative intensities are determined from atomic and instrument sensitivity factors.[58,59]

ATR-FTIR of the zirconated template indicates that the octadecylphosphonate molecules in the template layer are close packed. The IR spectrum from 3100 cm^{-1} to 2600 cm^{-1} for the template is shown in Figure 3.5 (top), and three bands are resolved.[13,55] The asymmetric methyl stretch ($\nu_a(CH_3)$), at 2958 cm^{-1}. The asymmetric methylene stretch ($\nu_a(CH_2)$) at 2918 cm^{-1}, and the symmetric methylene stretch ($\nu_s(CH_2)$) at 2850 cm^{-1}. The appearance of the $\nu_a(CH_2)$ at 2918 cm^{-1} with a fwhm of 20 cm^{-1} is the same as

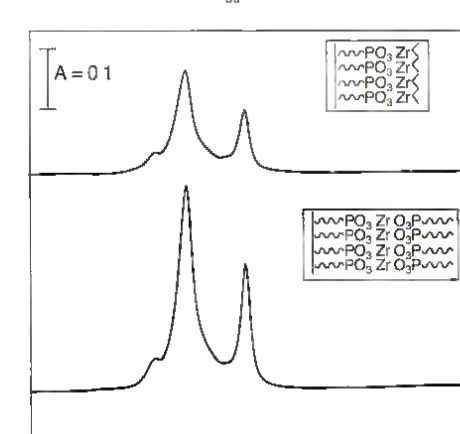

Figure 3-5 Infrared spectra of zirconium octadecylphosphonate films: zirconated LB template layer (top) self assembled octadecylphosphonic acid bilayer (middle), self-assembled octadecylphosphonic acid capping layer (bottom)

is seen in solid octadecylphosphonic acid [47] and indicates that the alkyl chains possess an all-trans conformation and are close packed. An increase in the number of gauche bonds will shift the $\nu_a(CH_2)$ to higher energy [13,55] while orientational disorder[13,55] will increase the fwhm.

Polarized ATR-FTIR[71,72] was used to determine the molecular axis tilt angles (from the normal) of the octadecylphosphonate molecules in the zirconated LB template layer. In this experiment the absorbance of the $\nu_a(CH_2)$ band was recorded with s- and p-polarized light. From the absorbance data, a dichroic ratio, D, defined as

$$D = (A_x + A_z)/A_y \qquad (3\text{-}1)$$

was calculated where $(A_x + A_z)$ is the absorbance with p-polarized light and A_y is the absorbance with s polarized light. The molecular axis tilt angles are determined from the dichroic ratio[71,72] listed in Table 3-2 and illustrated in Figure 3-6. The tilt angle for the zirconated LB template is 31°. This is precisely the tilt angle predicted from a SYBYL molecular modeling structure of zirconium octadecylphosphonate.[47] In the model, the crystallographic co-ordinates for α–$Zr(HPO_4)_2 \cdot H_2O$[33] are used to model the Zr O_3P binding, and alkyl chains are grafted on in place of the phosphate OH groups. The tilt angle results from the P-C bond orienting perpendicular to the zirconium ion planes.

Table 3-2. Polarized ATR Data for Zirconium Octadecylphopshonate Films

Film Type	Dichroic Ratio[a]	Tilt Axis[b]
Zirconated LB Template Layer	1.08	$31^0 \pm 5^0$
SA Capping Layer	1.0	$22^0 \pm 5^0$
LB Capping Layer	0.92	$5^0 \pm 5^0$

a. Dichroic Ratio is defined as $(A_x + A_z)/A_y$. b. Tilt angle is defined as the tilt of the molecular axis with respect to the surface normal.

The large tilt angle observed for the LB template layer suggest that this layer relaxes in the pure water subphase after it is transferred. Addition of zirconium ions then cross-links the layer and holds it in place. Together XPS and ATR-FTIR analyses reveal that the zirconated LB template layer consists of a high-density of evenly-spaced Zr^{4+} sites on an organized octadecyl-phosphonic acid surface. The low solubility of zirconium phosphonates allows this layer to be used in subsequent assembly steps without loss of organic film or displacement of zirconium ions.

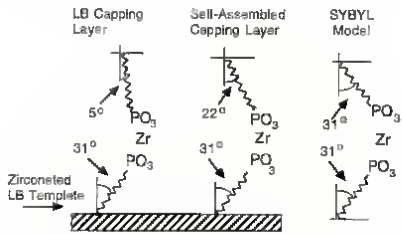

Figure 3-6 Molecular axis tilt angles for zirconium octadecylphosphonate films

Self-Assembly of Monolayers

Octadecylphosphonic acid is assembled to the zirconated LB template according to Figure 3-7 completing the zirconium octadecylphosphonate bilayer. The zirconated surface is placed into a 1.25mM (90/10 EtOH/H_2O) solution of the acid for 1 hr and then removed, rinsed and air dried. Figure 3-5

compares the infrared spectra zirconated LB template layer (top), the bilayer (middle) and the self-assembled octadecylphosphonic acid layer (bottom). The frequency and fwhm of each of the C-H stretching bands are the same in each spectrum indicating that the conformational order and packing density of the alkyl chains in the film are preserved after the SA step. The IR intensities in the bilayer spectrum are double those of the template spectrum indicating that the self-assembled layer contains the same amount of octadecylphosphonate as the zirconated LB template layer. This is further seen by comparing the top spectrum to the bottom spectrum in Figure 3-5, which is obtained by ratioing the self-assembled bilayer spectrum to the zirconated template layer spectrum. The frequencies, intensities, and peak shapes of the self-assembled layer are identical to those of the zirconated LB template layer, showing that the self-assembled layer is essentially equivalent to the LB layer.

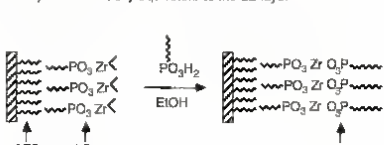

Figure 3-7 Self assembly of octadecylphosphonic acid at the Zr^{4+} LB template

The results of XPS analyses on the self-assembled octadecylphosphonic acid bilayer are listed in Table 3.1. For comparison, Table 3-1 also contains XPS data from an octadecylphosphonic acid bilayer formed by capping the zirconated LB template with another LB layer of octadecylphosphonic acid.[47] The observed Zr:P ratio corrected for the photoelectron attenuation

lengths[28,57 60,62 63] for the self assembled bilayer is 1:2 within experimental error.[58,59] The same ratio is found when capping the template with an LB film[47] and is consistent with the stoichiometry of bulk zirconium phosphonates.[33,62] The Zr:P ratio supports the infrared data and shows that each Zr^{4+} site in the template binds an octadecylphosphonic acid molecule from solution.

Contact angle measurements (Figure 3-6) on the self-assembled bilayer result in an advancing contact angle of 110° ± 1°, which is lower than the 112° contact angle observed when the zirconated LB template layer is capped with a second octadecylphosphonic acid LB monolayer.[47] Tilt angles of the alkyl chains, derived from polarized ATR-FTIR,[71,72] are listed in Table 3-2 and shown in Figure 3-6. The tilt angles for the self-assembled and LB octadecylphosphonic acid capping layers are 22° and 5°, respectively. The 5° tilt angle of the LB capping layer is consistent with X-ray diffraction data from LB multilayers of zirconium octadecylphosphonate.[47] This nearly perpendicular arrangement of the alkyl chains accounts for the higher contact angle relative to the self-assembled layer. The surface pressure used to align the molecules in the LB experiment orients the alkyl chains nearly perpendicular to the surface,[47] and it appears that this packing is preserved when the layer is transferred to the zirconated LB template layer. Once the zirconium-phosphonate bond is formed, this extremely strong binding interaction does not allow the LB capping layer to relax. Since there is no pressure applied when binding the self-assembled layer, this layer does not orient perpendicular to the surface. The higher tilt angle observed for the self-assembled capping layer is quite reasonable given the size of the phosphonate head group, and is similar to the orientation of the alkyl chains seen in solid state zirconium alkylphosphonates.[33,62] In fact, the bilayer formed by self assembling the capping layer is closer to a single-layer

analog of the oil the solid-state zirconium phosphonates than the bilayer formed by LB methods alone

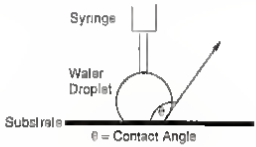

Figure 3-8 Contact angle measurement schematic

Self-Assembly of Multilayered Films

Mallouk and coworkers[2,24,27,29] have demonstrated that the Zr-phosphonate interaction can be used to build multilayer films. We followed their procedure for depositing 1,10-decanediyldiphosphonic acid (DDPA) to build multilayer films of the zirconated LB template (Figure 3.9). A substrate coated with the zirconated LB template layer is placed into a 1.25mM aqueous solution of DDPA for 1 hr. The substrate is then rinsed with water and multilayers are assembled by alternately repeating the Zr^{4+} ion and DDPA depositions.[24,25] The layer-by-layer deposition was monitored by ATR-FTIR and Figure 3.10 shows the C-H stretching region of the zirconated LB template layer (top), the template-DDPA bilayer (middle), and the self-assembled DDPA layer (bottom). The $\nu_a(CH_2)$ for the template-DDPA bilayer appears at a frequency of 2920 cm^{-1} and possesses a fwhm of 34.7 cm^{-1}. The increase in frequency and fwhm seen in the bilayer spectrum relative to the zirconated LB template layer indicates that more gauche bonds[13,55] are present in the bilayer, and that the film is no longer

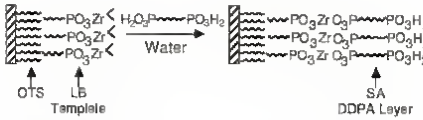

Figure 3.9 Self assembly of DDPA at the zirconated LB template layer

close packed [13,56] The bottom spectrum in Figure 3-10 is the DDPA layer only, which is obtained by ratioing the template-DDPA bilayer spectrum to the template layer spectrum. The DDPA IR spectrum indicates that this layer is disorganized The frequency and fwhm of the $\nu_a(CH_2)$ are 2924 cm^{-1} and 41 cm^{-1} respectively which are similar to the $\nu_a(CH_2)$ values obtained from a solution spectrum of octadecylphosphonic acid [47] and correspond to a large percentage of gauche bonds[13,55] and loose packing of the alkyl chains [13,56]

A plot of the integrated area of the $\nu_a(CH_2)$ versus the number of layers of assembled DDPA (Figure 3-11) shows a nonuniform increase in area with an increasing number of layers The integrated area of the $\nu_a(CH_2)$ for the first DDPA is much larger than the subsequent layers, although, after the fourth layer the increase in area with each additional DDPA layer becomes constant Figure 3.11 also represents a plot of the fwhm for each individual DDPA layer The fwhm decreases with the first four layers until it reaches a constant value of 34.7 cm^{-1} The IR data suggest that once a DDPA molecule binds one end to the template layer the exposed phosphonic acid group is able to bend over and bind another Zr^{4+} ion site within its reach, which is a consequence of the high density of Zr^{4+} ion binding sites and the fact that DDPA is not a rigid molecule The bridging of the Zr^{4+} ion sites by the DDPA molecules limits the number of sites available for binding in subsequent layers and accounts for the smaller

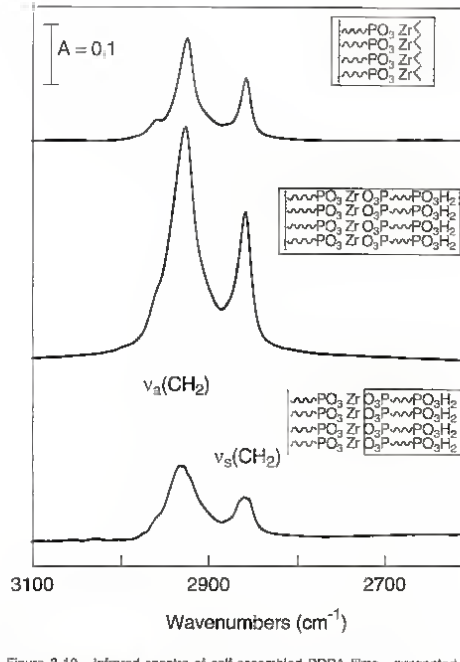

Figure 3-10 Infrared spectra of self assembled DDPA films: zirconated LB template layer (top); self-assembled DDPA bilayer (middle) and only the DDPA capping layer (bottom)

increase in area of the $\nu_a(CH_2)$ for each additional layer. After the fourth layer, however, a constant increase in area is observed, and the organization of each layer as determined by the $\nu_a(CH_2)$ lineshape, also becomes regular. At this point, it seems that the remaining available Zr^{4+} binding sites are spaced in such a manner that the bridging of these sites by the DDPA molecules is now less likely, and each subsequent assembly cycle deposits a constant amount of material resulting in the layer by layer deposition observed by other workers[2,24,25]. However, the overall nonlinear increase in the area, coupled with the shape of the $\nu_a(CH_2)$ stretch, indicates that the film is not well ordered.

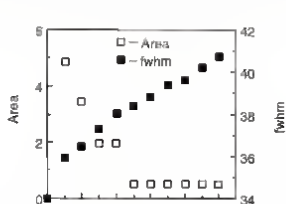

Figure 3-11. Infrared analysis of DDPA layers self assembled at the zirconated LB template.

The deposition of DDPA at the zirconated LB template was also monitored by ellipsometry. A plot of the thickness for each DDPA layer assembled at the zirconated LB template is shown in Figure 3-12. The thickness is determined for the overall thickness of each layer added to the film. The large initial thickness is due to the oxide layer, an OTS monolayer, and the zirconated LB template on the surface. The data were fit using a refractive

index of 3.94 for the Si substrate and 1.55 for the DDPA film. The data indicate that the first few layers result in a smaller increase in thickness than the latter layers assembled. The nonlinear increase in thickness supports the idea that the DDPA molecules bridge the Zr^{4+} ions at the zirconeled LB template until the Zr^{4+} ions are spaced such that the DDPA molecules can no longer bridge the Zr^{4+} sites. However, the increase in thickness for each individual layer after the first few layers is much larger than the predicted length of the DDPA molecule. Experimentally, the thickness per DDPA layer was determined by Mallouk[25] to be 17 Å, whereas a calculated length of the DDPA molecule, depending on the bond lengths[12,62] chosen and the tilt angle of the alkyl chain, ranges between 19-20 Å. Our data demonstrates that the average thickness per layer, which is 26 Å ± 6 Å, after the first few layers assembled is much larger than expected. In these type of films a poor estimation of the refractive index can lead to an overestimate in the thickness of the films.[43] It seems reasonable that if all of the Zr^{4+} sites are not bound by DDPA molecules then the assumed refractive index of 1.55, estimated for an organic surface, is incorrect. However, the fact that there is a change in the slope of the thickness measurements near the same number of layers as the change in slope for the infrared analysis supports the idea of DDPA molecules bridging to the zirconeled template.

Self Assembly of Rigid Molecules

To avoid the possibility of bridging surface sites by the α,ω-diphosphonic acid molecules, we investigated layer-by-layer depositions of a rigid diphosphonic acid, quaterthiophenediphosphonic acid (QDP) developed by Katz.[40] Katz and co-workers[40] have shown that QDP can be self assembled in a similar manner as the α,ω-alkyldiphosphonic acid molecules. QDP is easily

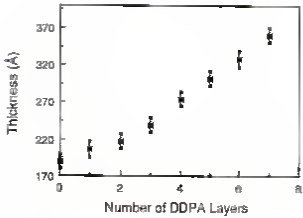

Figure 3-12 Ellipsometric measurements for DDPA self-assembled at the zirconated template layer

self-assembled at the zirconated LB template from a 1mM 50/50 DMSO/H_2O solution of QDP that is adjusted to a pH = 3 with a 10% solution of HCl. Depositions are carried out at 25° C for 1 hr and then the films are rinsed with a 50/50 DMSO/H_2O solution followed by a second rinse with pure water to remove any excess material. Previous work[40] involving the self-assembly of QDP indicated that elevated temperatures were needed to overcome steric barriers, although the data below demonstrate that QDP molecules can be self-assembled at room temperature. The difference may be that the close-packing of the LB layer prohibits any of the surface groups from being buried in the organic layer, thereby allowing the QDP molecules to access more Zr^{4+} sites at the surface.

The layer-by-layer assembly of QDP was monitored by UV-vis spectroscopy with the incident beam perpendicular to the substrate. There is no change in the UV-vis spectrum when the time of deposition is increased, suggesting that the deposition is complete after 1 hr. This is confirmed by XPS

which shows that for deposition times of 1 hr and 7 hrs the Zr:P S ratios are the same within experimental error [58,59]. A plot of the UV-vis absorbance of the λ_{max} at 390nm versus the number of QDP layers self-assembled at the zirconated LB template is shown in Figure 3-13.

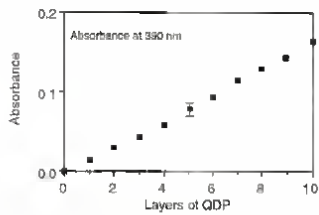

Figure 3-13. UV-vis absorbance versus the number of QDP layers self-assembled at the zirconated LB template.

The linear increase in absorbance demonstrates that the same amount of QDP is deposited during each cycle. The UV-vis absorbance per QDP layer is less than what has been previously reported [40]. The transition moment for the 390 nm band is parallel with the molecular axis [83,84] and the lower absorbance in the transmission experiment is consistent with the average orientation of the QDP molecular axis approaching the surface normal.

Figure 3-14 shows XPS multiplex spectra for a single layer of QDP self-assembled onto the zirconated LB template. From an XPS survey scan, C, O, P, S, Zr and Si (from the substrate) are the only elements present at the surface. The multiplex spectrum reveals a Zr:P:S ratio of 1 : 2.5 : 3.2. A model was

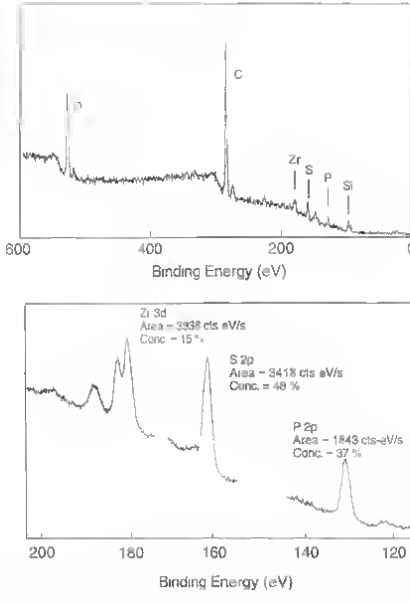

Figure 3-14 XPS spectra of a QDP monolayer self-assembled at the zirconated LB template layer. The top spectrum is a survey scan of the layer and the bottom spectrum is a multiplex scan for the binding energy region containing Zr, P, and S atoms.

derived from the attenuation equation[57] in order to predict the relative elemental intensities of Zr P and S in the sample. The attenuation equation defined as

$$I_A = I_A^{\infty}\exp(-d_m/(\lambda_m \sin\Theta)) \qquad (3\text{-}2)$$

was discussed in chapter 2. The distance of each element from the outermost surface is calculated from known interatomic distances[48,61] assuming vertical orientation of the QDP molecules with respect to the substrate plane. For 100 % coverage i.e. one template Zr^{4+} ion binds one QDP molecule, one expects a Zr P S ratio of between 1.0 : 3.8 : 5.5 and 1.0 : 3.1 : 4.2 for low[60] and high[25,30] values of λ_m, respectively. These ratios are not observed and we conclude that our reported Zr P S ratio of 1 : 2.5 : 3.2 is consistent with a QDP coverage of approximately 50 % to 60 % depending upon the value of λ_m chosen. In addition, as an internal check, the relative ratio of P to S is consistent with QDP adsorbing to the surface without trapping excess DMSO in the film. The incomplete coverage of the QDP molecules is perhaps explained by the mismatch between the cross-sectional molecular areas of the Zr^{4+} ion sites and the QDP molecules. The area per binding site for the zirconated LB template is dictated by the cross-sectional area per molecule of the LB octadecylphosphonic acid film[46,47] which is 24 $Å^2$ whereas the calculated cross-sectional area for the QDP molecule[35] is approximately 28 $Å^2$.

X-ray diffraction from ten layers of QDP assembled at the zirconated LB template is shown in Figure 3-15. The experimental data are fit by superimposing two Lorentzian peaks onto a background that was modeled by the sum of a zero-point Lorentzian plus a quadratic contribution due to diffuse scattering. The peak at a 2θ value of 4.37° can be assigned to the (001) reflection and corresponds to a d-spacing of 20.19 Å. A second order reflection

is also seen. The d-spacing for the QDP multilayers film agrees well with the size of the QDP molecule.[40] If the QDP molecules are oriented exactly perpendicular to the surface a d-spacing of 21 Å is predicted.[40] The observed d-spacing suggest that the QDP molecules are slightly tilted from the surface normal.

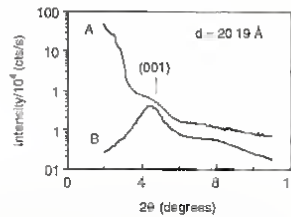

Figure 3-15. Low-angle x-ray diffraction from ten layers of QDP self assembled at the zirconated template layer. A is the experimental data and B is the Lorentzian fit of the data.

The inter-layer coherence length (L) can be estimated using the Scherrer formula.[58]

$$L = 0.94\lambda/(B(2\theta)\cos\theta_B) \qquad (3\text{-}3)$$

where λ is the wavelength of the X-ray, B(2θ) measured in radians is the fwhm of the 2θ peak, and θ_B is the Bragg angle for the peak. Using a fwhm of 0.0109 radians, taken from the fitted data for the (OQ1) reflection, a coherence length of 133 Å is obtained which corresponds to 6 or 7 layers. This is consistent with the broad (002) reflection and the Lorentzian lineshapes, and is reasonable for a

10-layer film if we consider that the first and last layers probably assume a different packing than the bulk. X-ray diffraction demonstrates that layered films can be produced using one-layer-at-a-time self-assembly deposition methods [27]. The close packed LB template layer appears to orient the QDP molecules nearly perpendicular to the surface such that well ordered layers can be assembled even though the mismatch in area between the Zr^{4+} sites in the zirconated LB template and the QDP molecules hinders the formation of a more organized film. It seems reasonable that by using a template molecule that results in a Zr^{4+} ion spacing closer to the QDP cross-sectional area a more crystalline film could result.

Summary

In conclusion, a zirconated octadecylphosphonic acid LB film provides an organized and well-defined surface for assembling organophosphonate molecules from solution. When octadecylphosphonic acid is assembled at the zirconated LB template, a zirconium phosphonate bilayer is formed with the self-assembled layer assuming a similar organization as the original LB template layer. The order of the template is transferred to the self-assembled layer. The bilayer formed by self-assembling octadecylphosphonic acid to the zirconated LB template provides a good single layer analog of layered solid-state zirconium phosphonates. Multilayers can also be produced at the LB template by self-assembling α,ω-diphosphonic acid molecules. If the diacid molecule is rigid, a well-defined layered structure can be produced. In the multilayers formed from QDP, the interlayer spacing, determined by X-ray diffraction, is comparable to the length of the QDP molecule. Because the zirconated LB surface is close packed and inflexible, the QDP packing density

is limited by the cross-sectional area of the QDP molecule. The incommensurate size of the LB template molecules and the QDP molecule however probably limits the in-plane order that can be achieved with this system. In the case of 1,10-decanediyldiphosphonic acid where the diacid molecule is flexible multilayer films can also be produced although the layered nature of these films is less well defined. Initially the flexible α,ω-diphosphonic acid molecules bridge Zr^{4+} sites in the template layer therefore reducing the density of binding sites available in subsequent layers. Finally a well characterized and organized LB template layer can play an important role in understanding and quantifying layer-by-layer self assembly. For applications where controlling the architecture, order and density of molecules within layered assemblies is required the organization of the template layer is important.

CHAPTER 4
TWO-DIMENSIONAL MAGNETISM: EVIDENCE FOR SHORT RANGE ANTIFERROMAGNETIC ORDER IN A LANGMUIR BLODGETT FILM

Introduction

The preparation of two-dimensional magnetic and electronic materials is becoming increasingly important in advanced materials. It has been reported that target densities of 10^{10} bits/cm^2 for high density recording media will require film thicknesses approaching a monolayer.[87] Recently, techniques have been developed to produce thin films of layered inorganic solids that exhibit properties such as superconductivity.[88] The quasi-two-dimensional structure of layered inorganic solids[3,4,89] makes them attractive experimental models for investigating chemistry and physics in the limit of two dimensions. These layered structures are termed "quasi" because although the structures are anisotropic, they are still part of a three dimensional crystal.

Thermodynamic considerations of magnetic exchange determine that a transition to long range order is not possible in a one dimensional chain.[90] An ordering transition for a two-dimensional system, however, is model dependent.[90-92] Magnetic ordering depends on the nature of the nearest neighbor exchange. This can be expressed as

$$\mathcal{H} = -2\Sigma\{J_{xy}(S_{ix}S_{jx} + S_{iy}S_{jy}) + J_zS_{iz}S_{jz}\} \qquad (4\text{-}1)$$

where J is the exchange constant and S is the spin on the atoms. For the Ising model ($J_{xy} = 0$) magnetic ordering is predicted in two-dimensions.[81,82] However, in the XY ($J_z = 0$) or Heisenberg ($J_{xy} = J_z$) models, magnetic ordering is not predicted.[80,82] In spite of the predictions, long range magnetic order has been observed in quasi-two-dimensional layered materials.[4,83] In these layered compounds, magnetic interactions between planes are assumed to be small compared to the magnetic interaction within a plane and are often ignored. At high temperatures this is a valid assumption, however, as the temperature is lowered the interplane coupling becomes increasingly more important.[80] A potentially better two-dimensional system is a true monolayer where the magnetic coupling is restricted to two-dimensions.

Single layers of atoms[5,8,84] and inorganic solids have been prepared on surfaces by either chemical vapor deposition or molecular beam epitaxy. However, these films often suffer as two-dimensional models because interactions between the substrate and the monolayer can dominate the physical properties of interest.[7] A different approach to creating a magnetic monolayer is to incorporate two-dimensional arrays of inorganic ions or complexes into organic monolayers. Experimental methods are now available to prepare monomolecular organic films one-layer-at-a-time. Recent advances in surface analysis techniques has led to the understanding of their molecular structure.[85] These preparative methods, such as Langmuir-Blodgett[10,12] (LB) and self-assembly[12,14] (SA) techniques[12,14] can be used to construct well-organized organic films which show promise as photoconductors[86] and nonlinear optical materials,[76] but have yet to meet expectations as magnetic materials. The first example of incorporating metal ions into an organic film for magnetic studies was reported by Pomerantz.[31,32] Pomerantz prepared LB films of manganese stearate, however, a transition to long range order was

never observed in these manganese stearate films. Our premise is that the best chance to prepare magnetic LB films begins with preparing LB films of known solid-state structures that undergo magnetic ordering. To this end, we have prepared LB films analogous to the manganese phosphonates.[37]

The manganese phosphonates[37] ($(RPO_3)Mn\ H_2O$) belong to a class of organic-inorganic layered materials (Figure 4-1). In these materials, the manganese ion planes are surrounded by phosphonate groups above and below the plane. Each manganese ion is bound by five oxygen atoms from the phosphonate groups and one water molecule that occupies the sixth coordination site.[37] The manganese phosphonates crystallize in an orthorombic space group and the bonding within the manganese ion plane is independent of the organic group.[37] We have demonstrated that the bulk manganese phenylphosphonate orders antiferromagnetically.[45] Therefore in an attempt to prepare a two-dimensional magnetic system, a method to prepare single and multilayered films of manganese octadecylphosphonate has been developed.

We present evidence that the LB films are structurally analogous to the bulk manganese phenylphosphonate. Magnetic studies indicate that the LB films can be viewed as two-dimensional magnetic systems. The magnetic data will show evidence for short range antiferromagnetic order in an LB film.

Experimental Section

Materials

Octadecylphosphonic acid ($C_{18}H_{39}O_3P$) was used as purchased from Alfa (Ward Hill, MA). Decylphosphonic acid ($C_{10}H_{23}O_3P$) was prepared by

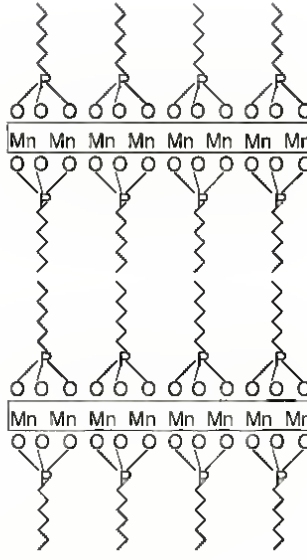

Figure 4-1. Idealize structure for manganese phosphonate The water molecules are not shown for clanty

Margaret L. Showalter[45] from commercial decylbromide using the Michaelis-Arbuzov[49] reaction followed by acid hydrolysis. Manganese chloride tetrahydrate ($MnCl_2{\cdot}4H_2O$) was used as purchased from Fisher Scientific (Orlando, FL). Manganese decylphosphonate ($C_{10}H_{21}O_3P$) Mn H_2O was prepared by following a procedure similar to that published by Mallouk and coworkers[37]. First 1.35 mmoles of $C_{10}H_{23}O_3P$ was dissolved in 50 ml of EtOH at 60° C. Once in solution 1.35 mmoles of $MnCl_2{\cdot}4H_2O$ were added to the solution. Sodium hydroxide (1M) was then added dropwise until a white precipitate formed. The mixture was allowed to stir at 60° C for 3 days. The white powder was filtered and rinsed 5 times with water and ethanol. Combustion analysis of the sample is as follows: Calcd: C, 40.95; H, 7.85. Found: C, 40.63; H, 7.89.

Substrate Preparation

Single crystal (100) silicon wafers purchased from Semiconductor Processing Company (Boston, MA) were used as deposition substrates. Silicon and germanium attenuated-total-reflectance (ATR) crystals, (50mm x 10mm x 3mm) purchased from Wilmad Glass (Buena, NJ) were used as substrates for all infrared experiments. Germanium ATR crystals were used to study the region from 1500 cm^{-1} to 900 cm^{-1}. The ATR crystals were parallelograms with a 45° angle of incidence with respect to the parallel faces. The silicon substrates were cleaned using the RCA cleaning procedure[50] then dried under N_2. Germanium ATR crystals were first washed with $CHCl_3$ then cleaned under an argon or oxygen plasma. Octadecyltrichlorosilane (OTS) coated surfaces were prepared by placing the cleaned substrates in a 2% solution of OTS in a solvent consisting of 80% hexadecane, 12% CCl_4, and 8%

$CHCl_3$ by volume for 2 hr. Substrates were then rinsed with chloroform to remove any excess hexadecane then dried under flowing N_2. Transmission electron microscope substrates were prepared by placing a copper grid (300 mesh) purchased from Ted Pella, Inc. (Redding, CA) onto a floating polyvinylformal (Formvar) layer. This was then transferred to a microscope slide. A second layer of Formvar was added and 300 Å of SiO was deposited on top of the formvar. The substrate was then made hydrophobic by the OTS procedure previously mentioned. The complete details of this procedure has been outlined in a paper by Fisher and Sachman.[51] For the EPR experiments, Mylar was chosen as a suitable substrate. Calcium arachidate (16 layers) was first transferred to the Mylar to prepare a smooth hydrophobic surface. The manganese octadecylphosphonate films were then transferred to the hydrophobic surfaces. The Mylar was cut into ≈ 2mm strips and placed into an EPR tube.

Instrumentation

The Langmuir-Blodgett experiments were performed using KSV Instruments (Stratford, CT) PFTE (teflon) coated LB troughs with hydrophobic barriers. A Barnstead NANOpure purification system produced water with a resistivity of 18 MΩ-cm for all experiments. Depositions were carried out using the KSV 3000 system with a home-built single or dual barrier attachment and in all cases films were compressed linearly at a rate of 8 mN/m/min at room temperature. A target pressure of 17 mN/m was maintained with deposition speeds of 8 mm/min for the down stroke and 5 mm/min for the up-stroke.

Infrared spectra were recorded with a Mattson Instruments (Madison, WI) Research Series-1 Fourier transform infrared (FTIR) spectrometer using a

narrow band mercury cadmium telluride detector A Harrick (Ossining NY) TMP stage was used for the ATR experiments

Advancing contact angle measurements were measured with a Rame-Hart (Mountain Lakes NJ) NRL Contact Angle Goniometer Model 100 00 A 250 mL syringe was used to dispense a fixed-volume water drop to the surface.

Ellipsometry measurements were obtained with a Rudolph Instruments Series 431A Universal Ellipsometer (Fairfield NJ) A He-Ne laser (632 8 nm) was used as the light source The angle of incidence was set at 70° for all experiments The parameters Ψ and Δ were estimated from the polarizer and analyzer settings The refractive index and thickness of the films were calculated using an in house computer program.

X-ray photoelectron spectra were obtained using a Perkin-Elmer (Norwalk CT) PHI 5000 Series spectrometer All spectra were taken using the Mg Kα line source at 1253 6 eV The spectrometer has a resolution of 2 0 eV with anode voltage and power settings of 15 kV and 300 W, respectively Typical operating pressure was 5×10^{-8} atm Survey scans were performed at a 45° take off angle with a pass energy of 89 45 eV Multiplex scans 140 scans at each peak, were run over a 20 to 40 eV range with a pass energy of 37 75 eV The observed relative intensities are determined from experimental peak areas normalized with atomic and instrument sensitivity factors [58 59]

Transmission electron microscopy (TEM) and diffraction (TED) experiments were preformed on a JEOL (Peabody MA) JEM 200CX electron microscope In all cases a 100 kV accelerating voltage was used Diffraction patterns were obtained at 30K 50K and 82K magnification The camera constant of 29 78 mm Å for the diffraction pictures was obtained from a titanium standard The sample was cooled to liquid nitrogen temperatures and the electron beam was normal to the sample

Results and Discussion

Deposition Procedure

The bulk divalent transition metal phosphonates[37,38] are normally prepared by precipitation from water. In a typical experiment, equal molar amounts of the phosphonic acid and transition metal are first dissolved in water and the pH is adjusted by NaOH to 5-6 causing the solid to form. We propose that under the appropriate conditions thin films of the divalent metal phosphonates can be prepared via the LB method. This idea is illustrated in Figure 4-2. Our hypothesis is that if the divalent metal is in the subphase and a phosphonic acid film is compressed on this subphase at a specific pH (pH = 5-6) then the metal ions would bind with the film at the air/water interface. The formation of a single-layer analog could then be accomplished by transferring a bilayer of the film-containing metal ions to a hydrophobic surface. Our premise is that during the transfer in the meniscus region all of the elements in the correct stoichiometry would be present to form a single-layer analogous to the solid state structure. The driving force for crystallizing the phosphonate structure would be a combination of the lattice energy of the solid and the draining of the water from the film. However, before the deposition is possible the behavior of the phosphonic acid Langmuir monolayer must be understood.

Phosphonic Acid Film on a Metal-Containing Subphase

In chapter 2 we described the behavior of octadecylphosphonic acid on a pure water subphase. Briefly the film possesses a cross-sectional area of 24 Å and collapses at a pressure of 60 mN/m. The octadecylphosphonic acid film

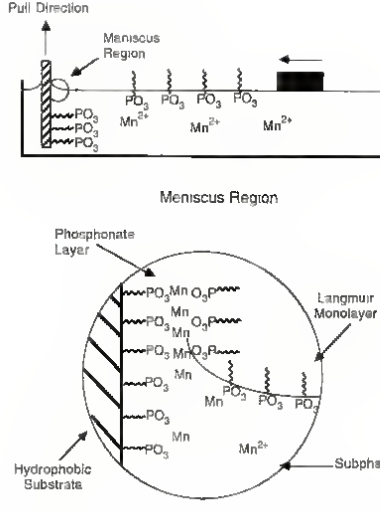

Figure 4-2 Deposition procedure for preparing manganese octadacyl-phosphonic acid LB films

also showed a creep of 0.5 mm/min which corresponds to a change in area of 47 mm^2/min. The isotherm of octadecylphosphonic acid compressed on a Mn^{2+} subphase (Figure 4-3) at a pH of 5.5 possesses a cross-sectional area of 27 Å but the increase in pressure is not as sharp and a collapse pressure is never reached. At a pressure of 40 mN/m the Wilhelmy plate is pushed from the vertical, therefore an accurate pressure measurement of the film is no longer possible. The movement of the Wilhelmy plate is interpreted as strong binding between the Mn^{2+} ions and the phosphonic acid film which is indicative of a rigid film.[46,47]

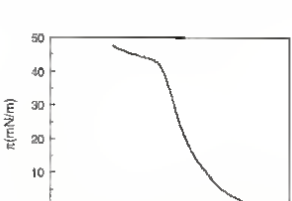

Figure 4-3. Octadecylphosphonic acid isotherm compressed on a Mn^{2+} ion subphase at a pH of 5.5. The film was compressed using a single-barrier trough.

Hysteresis experiments (Figure 4-4) suggest that the metal ions bind to and stabilize the octadecylphosphonic acid film. In this experiment the octadecylphosphonic acid film is compressed to a specific cross-sectional area and then immediately decompressed. In Figure 4-4 only the compressions are shown for clarity. As the film is repeatedly compressed over the Mn^{2+} ion

subphase. The cross-sectional area increases. The increase in cross-sectional area is different than that observed when octadecylphosphonic acid is formed on a pure water subphase, where the cross sectional area of the film decreases upon repeated compressions. The increase in cross-sectional area suggests that the metal ions are incorporating into the film at the air/water interface. The increase in cross sectional area also suggests that film does not dissolve into the subphase [46,47]

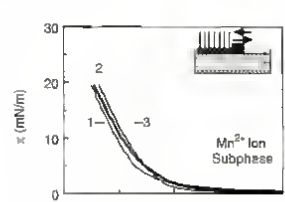

Figure 4-4 Hysteresis experiment of octadecylphosphonic acid compressed on a Mn^{2+} ion subphase at pH = 5.5

To measure the stability of the film the change in area of the octadecylphosphonic film over a period of time is monitored. In this experiment (Figure 4-5) the octadecylphosphonic acid film is compressed to a pressure of 20 mN/m which is maintained for 1 hr and then the film is decompressed. Figure 4-5 shows the change in barrier movement which is directly related to the area as a function of time. An increase in barrier movement corresponds to the molecules being compressed into a close packed film. While the pressure is being maintained the change in area can be related to the stability of the film

The slope of the barrier movement is small while the pressure is held constant at 20 mN/m which indicates that the film does not readily dissolve into the subphase. After four compressions the slope of the barrier movement at constant pressure is equal to zero which is indicative of a rigid film. We interpret this as the Mn^{2+} ions cross linking the phosphonate groups at the air/water interface.

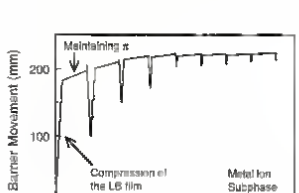

Figure 4-5 Hysteresis of octadecylphosphonic acid on a Mn^{2+} ion subphase with a 1 hour delay

Deposition of Manganese Octadecylphosphonate

Deposition of the manganese octadecylphosphonate is accomplished by using the Langmuir Blodgett vertical deposition method [10,12]. In a typical deposition (Figure 4-2) experiment octadecylphosphonic acid is compressed over a Mn^{2+} ion subphase to a pressure of 17 mN/m. At this point, an OTS-covered substrate is lowered through the film at the air/water interface, thereby transferring the film in a tail-to-tail or hydrophobic fashion. Once the first layer is deposited, the substrate is then raised from the subphase through the film creating a head-to-head or hydrophilic interaction. This hydrophilic interaction

occurs in the region where the inorganic extended lattice will be formed. In this procedure the deposition speed for the up-stroke is likely to be critical. A slow deposition speed and thus a slow draining of the water from the film should aide in the crystallization of the inorganic lattice. We have found that 5 mm/min is the optimum speed for transfer. The pH of the subphase also effects the transfer of the monolayers and the optimum pH for deposition is 5.2-5.5.

Multilayers of the manganese octadecylphosphonate cannot be formed by continuous deposition of the film due to cross-linking of the manganese ions with the phosphonate groups at the air/water interface. In order to prepare multilayered films a new octadecylphosphonic acid monolayer must be prepared after the first bilayer is transferred. This deposition technique produces continuous films with a transfer ratio of unity. Contact angles of 110° ± 1° for the multilayered films confirm that continuous films are prepared.

Structural Analysis of Manganese Octadecylphosphonate

Infrared analysis

The infrared spectra of Langmuir-Blodgett films can be used to elucidate information about the order[13,55] and packing[13,56] of the alkyl chains as well as derive information about the composition of the film. If the Mn^{2+} ions are bound to the phosphonic acid molecules as the isotherms suggest, the P-O stretching[57,58] region from 1100-900 cm^{-1} should differ for the octadecylphosphonic acid and manganese octadecylphosphonate films. Figure 4-6 compares the infrared spectrum of an octadecylphosphonic acid bilayer (top) and a manganese octadecylphosphonate bilayer (bottom). In both spectra the common bands are [13,55] the asymmetric methyl stretch ($\nu_a(CH_3)$), at 2958 cm^{-1} the asymmetric methylene stretch ($\nu_a(CH_2)$) at 2917 cm^{-1} the

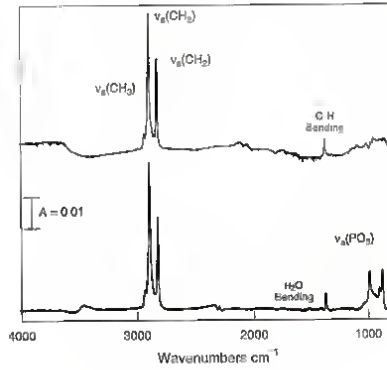

Figure 4 6 Infrared spectra of octadecylphosphonic acid (top) and manganese octadecylphosphonate LB films (bottom)

symmetric methylene stretch ($\nu_s(CH_2)$) at 2850 cm^{-1} and the methylene bending mode at 1467 cm^{-1}. However in the manganese octadecylphosphonate bilayer spectrum (bottom) additional bands are resolved [97,99] the asymmetric phosphonate stretch ($\nu_a(PO_3^{2-})$) at 1085 cm^{-1} the symmetric phosphonate stretch ($\nu_s(PO_3^{2-})$) at 975 cm^{-1}, the O-H stretch at 3474 cm^{-1} and the H_2O bending mode at 1608 cm^{-1}. The P-O and water bands are observed in the bulk divalent metal phosphonates [38,39].

The frequency and full-width-at-half maximum (fwhm) of the $\nu_a(CH_2)$ are used to determine the conformational order[13,55] and packing[13,55] of the aliphatic chains in LB films. The $\nu_a(CH_2)$ appears at 2917 cm^{-1} which indicates the the alkyl chains are in an all-trans conformation. The fwhm of the $\nu_a(CH_2)$ is 15.4 cm^{-1} for both films which suggests that the alkyl chains are close packed. In contrast, zirconium octadecylphosphonate films posses[46,47,100] a fwhm of 20 cm^{-1}. The difference in fwhm indicates that the manganese phosphonate films are more well ordered and crystalline than the zirconium phosphonate films. Plotting the increase in area of the $\nu_a(CH_2)$ and the $\nu_s(CH_2)$ stretches as a function of the number of bilayers (Figure 4-7) shows a linear increase in area for both bands. This indicates that the same amount of material is being deposited after each cycle in the deposition process. The frequency and fwhm of the $\nu_a(CH_2)$ does not change with the increase in layers which suggest that the order of the alkyl chains is maintained. This is further substantiated by the fact that the ratio of the peak areas for the $\nu_a(CH_2)$ band and the $\nu_s(CH_2)$ band is constant throughout the depositions.

The difference in the octadecylphosphonic acid film and manganese octadecylphosphonate film is clearly demonstrated in the P-O region. The asymmetric and symmetric PO_3^{2-} stretches[97,99] are observed only in the film

compressed over a Mn^{2+} subphase (Figure 4-6). This indicates that the phosphonic acid groups are ionized which is attributed to the Mn^{2+} ions binding

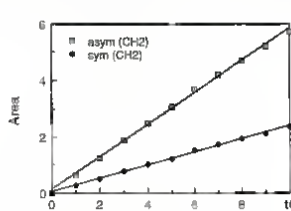

Figure 4-7 A plot of the area of the methylene bands versus the number of bilayers of manganese octadecylphosphonate

the phosphonate groups in the transferred film. The absence of the strong P=O stretch[97,98] in the 1350-1250 cm^{-1} region or the 1250-1110 cm^{-1} region for free and hydrogen bonded modes respectively suggest that the all of the phosphonate groups in the film are ionized. The appearance of the H-O-H bend[99] at 1608 cm^{-1} also indicates that Mn^{2+} ions are present in the deposited films. In the bulk manganese phosphonates each Mn^{2+} ion is bound by five oxygen atoms from the phosphonate anion and one H_2O molecule fills out the coordination sphere.[95,97] Therefore, the presence of the H_2O bend (1608 cm^{-1}) along with the PO_3^{2-} stretches suggest that the LB film is analogous to the bulk manganese phosphonate structure.

Plotting the areas of the asymmetric PO_3^{2-} stretch and the H_2O bend as a function of bilayers (Figure 4-8) further demonstrates that the LB film is

structurally analogous to the bulk manganese phosphonate. For both bands the increase in area is linear with an increasing number of bilayers. This is evidence that the composition of the film is maintained throughout the deposition process and that water is incorporated into the LB film stoichiometrically.

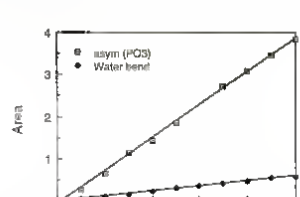

Figure 4.8. A plot of the asymmetric PO_3^2 stretch and the H_2O band versus the number of manganese octadecylphosphonate bilayers.

Ellipsometry

Ellipsometric measurements show a linear increase in thickness with an increasing number of bilayers (Figure 4-9). The thickness of each bilayer is calculated assuming a refractive index of 3.84 for the Si substrate and a refractive index of 1.544 for the LB film. The linear increase in thickness suggests that the same amount of material is being deposited after each deposition cycle. This result is consistent with the infrared and transfer ratio data. The solid line shown in Figure 4-9 is a linear regression fit of the data. From the slope of the regression line, a thickness per bilayer of 53 Å ± 5 Å is

obtained The initial thickness is due to a layer of oxide on the silicon substrate and an OTS layer

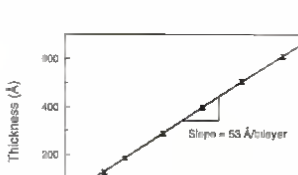

Figure 4-9 Ellipsometric data for manganese octadecylphosphonate

XPS analysis

Survey scans of single-bilayer and multilayered manganese octadecyl-phosphonate films show that C, O P and Mn are the only elements present within the film From multiplex spectra the ratio of the observed relative intensity for Mn P is 2 3 within 10 % error[58 59] However there is a 1:1 stoichiometry observed in the bulk solids The differences between the observed relative ratio in the film and the ratio of the bulk solid can be explained by the attenuation[57] of electrons by the overlayer In the XPS experiment, each element will contribute to the spectrum an area I_A defined as

$$I_A = I_A^{\infty}\exp(-d_m/(\lambda_m \sin\Theta)) \qquad (4\text{-}2)$$

in which I_A^{∞} is the peak area normalization or sensitivity factor[58] d_m is the overlayer thickness of material m in this case the octadecyl-phosphonate layer

λ_m is the inelastic mean free path of the photoelectron through material m and Θ is the take off angle with respect to the surface parallel. The relative intensities depend on the distance the element is from the surface and the mean free path (λ_m) of the electron. In the manganese octadecylphosphonate film the distance for Mn and P atoms from the surface differs by ≈ 2 Å however λ_m of the electrons are 26.9 Å for Mn atoms and 36.7 Å for P atoms. The λ_m for Mn and P are calculated from an equation developed by Seah and Dench[56] for organic films. This large difference in λ_m between the Mn and P atoms accounts for the M:P ratio of 2.3 that is observed in the films. The electron escape distance for the Mn atoms is smaller than the escape distance for the P atoms which causes a larger attenuation of the Mn peak relative to the P peak. We have used the attenuation equation[57] (4-2) to calculate the expected ratio of Mn:P intensities in an LB film assuming a 1:1 Mn:P stoichiometry and a layered structure. Table 4-1 compares the calculated Mn:P ratio with the experimentally observed Mn:P ratio of the LB film. The XPS data indicate that even though the observed ratio of Mn:P are 2:3, the stoichiometry is consistent with the bulk manganese phosphonate solid within experimental error.[58,59]

Table 4-1 XPS analysis of manganese octadecylphosphonate films

Manganese Octadecylphosphonate LB Films	Calculated Relative Intensities		Observed Relative Intensities	
	Mn	P	Mn	P
One Bilayer	40.19	59.81	37.25	62.75
Three Bilayers	39.19	60.81	35.70	64.30
Five Bilayers	39.16	60.84	42.50	57.50
Seven Bilayers	39.13	60.87	38.76	61.24

Calculated relative intensities were obtained from the attenuation equation.[57]

Transmission electron diffraction

Transmission electron diffraction (TED) can be used to determine the packing and in-plane order of Langmuir Blodgett films.[73,75,101] In this technique (Figure 4-10) electrons are directed perpendicular to the substrate surface. Most of the electrons pass through the sample unhindered, however, some of the electrons will be diffracted by a crystalline sample. The diffraction pattern can be analyzed to elucidate the unit cell parameters of the film.

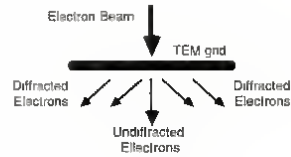

Figure 4-10. Transmission electron diffraction (TED).

Substrate preparation is crucial in obtaining a sample suitable for the TED experiment. We have followed the preparation method developed by Fisher and Seckman[51,101] which is illustrated in Figure 4-11. Briefly, an electron microscope grid (300 mesh) is fixed to a glass slide by 300 Å Formvar layer. A 300 Å layer of SiO is then evaporated onto the formvar. The slide is made hydrophobic by self-assembling OTS. Once the surface is made hydrophobic the LB film can be easily transferred to the glass substrate and thus the TED grid. The TED grid containing LB film is then pulled off the slide and placed in the instrument.

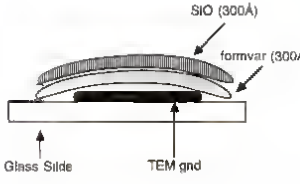

Figure 4-11 Substrate preparation of the transfer of an LB film to a TEM grid

The in-plane structure of a ten-bilayer manganese octadecylphosphonate LB film gives rise to a diffraction pattern of sharp rings (Figure 4-12). In typical LB films, the diffraction pattern is usually short-lived (less than 20 sec) because the electrons destroy the film. In contrast, the diffraction patterns we observe for the manganese octadecylphosphonate films possess a longer life-time (1-2 minutes) before eventually fading away. We believe that the longer life-time is due to diffraction from the inorganic planes. The d-spacings determined from Figure 4-12 are listed in table 4-2 along with the in-plane unit cell parameters. The unit cell parameters are compared to the manganese organophosphonate analogs which crystallize in an orthorombic space group.[37] We have assigned three distinct series of reflections d_{110}, d_{120} and d_{300} consistent with the bulk manganese phosphonates. The d-spacings from the LB film could not be assigned to any other manganese species that might be present in the subphase nor with a hexagonal lattice[73-75,101] usually associated with LB films. The TED analysis coupled with the infrared and XPS analyses demonstrates that the LB manganese octadecylphosphonate film is chemically and

Figura 4-12 Electron diffraction pattern from a ten-bilayer manganese octadecylphosphonate LB Film. The hkl reflections observed are the110 (first ring), the 120 (second ring), and the 300 (third ring)

structurally analogous to the known solid-state manganese phosphonate structures.[37]

Table 4-2 The d spacings and unit cell parameters for the manganese octadecylphosphonate LB films based on an orthorombic unit cell.

LB Film		In-Plane Unit Cell Parameters of Manganese Organophosphonates		
d-spacing	hkl	LB Film (± 0.05 Å)	Phenyl[a] analog	Methyl[a] analog
3.72 Å	110	a = 5.70 Å	a = 5.73 Å	a = 5.82 Å
2.27 Å	120	b = 4.94 Å	b = 4.85 Å	b = 4.91 Å
1.93 Å	300			

a Obtained from Mallouk *et al*.[37]

Magnetism in Manganese Octadecylphosphonate LB Films

Two-dimensional system

Whether or not a low dimensional magnetic system is expected to undergo a transition to long range order depends on the dimensionality of the lattice and the type of nearest neighbor exchange.[90-92] For example, a two-dimensional lattice with Heisenberg exchange is not expected to order magnetically, however, in some Heisenberg quasi two dimensional layered compounds a transition to long range order is observed. The ordering is believed to be due to either a 2D-3D crossover where the interplane exchange becomes important or a Heisenberg to Ising crossover where $J_{xy} << J_z$.[93] Both types of crossovers occur a low temperatures an can lead to a magnetically ordered state.[93] In an attempt to understand magnetic exchange in two-dimensions, we have prepared a multilayered analog of a known layered material by the LB method. One advantage of the LB method is that the magnetic planes can be separated by a large distance eliminating the 2D 3D

crossover For example the manganese planes in the manganese octadecylphosphonate LB film are separated by ≈ 53 Å ± 5 Å This large distance between magnetic planes should effectively eliminate interplane coupling because J(interplane) varies as r^{-3}, where r is the interplanar distance.[102] Pomerantz[31,32] and others[103] have suggested that LB films can be viewed as two dimensional magnetic systems His study of manganese stearate[31,32] demonstrated that the LB film possesses a two-dimensional magnetic anisotropy although a transition to long range order was never observed We want to observe how the magnetic exchange within monolayers differs from a known solid state structure Electron paramagnetic resonance spectroscopy (EPR) is the method of choice to study the magnetic properties of the LB manganese octadecylphosphonate films The advantage is the sensitivity of this technique which allows LB films to be probed.

The dependance of the EPR linewidth on the orientation of the sample with respect to the external field can be used to probe the magnetic dimensionality of the material.[32,104,105] The EPR linewidth is a function of the angle Θ of the magnetic field with respect to the magnetic ion planes For a quasi-two-dimensional system Richards and Salamon[105] demonstrated that the linewidth dependance is determined by

$$\Delta H = A + B(3\cos^2\Theta - 1)^2 \qquad (4\text{-}3)$$

where ΔH is the EPR linewidth and A and B are constants This dependance has been observed in quasi two-dimensional solid-state materials such as the alkylammonium layered perovskites[104] $(RNH_3)_2MX_4$ K_2MnF_4[104] and in LB films of manganese stearate.[32] Figure 4-13 shows the linewidth versus orientational dependance data for the LB manganese octadecylphosphonate film A best fit

of the data was obtained for A = 281G and B = 14 5 G The fact that the linewidth orientational dependence is fit by equation 4-3 suggests that the manganese octadecylphosphonate LB film is a two-dimensional magnetic system

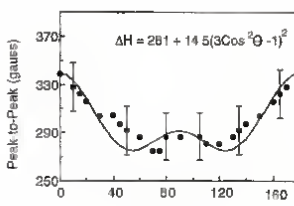

Figure 4-13 EPR linewidth as a function of orientation for a manganese octadecyiphosphonate LB film

Evidence for short-range antiferromagnetic order

The manganese octadecyiphosphonate LB film is expected to be a Heisenberg magnetic system.[32] The manganese (II) ion is a S state ion in the ground state The orbital angular function of a S-state ion in three dimensions is spherical and is considered isotropic Evidence for cooperative magnetic phenomena is observed by monitoring the EPR linewidth dependence as a function of temperature.[32,104] For a two dimensional antiferromagnet,[32,104,105] the linewidth increases dramatically near the transition temperature (T_N). This is due to a decrease in the relaxation time as antiferromagnetic exchange goes from short range to longer range order For the manganese octadecyl-phosphonate LB film the linewidth gradually broadens as the temperature is

lowered from 298 K (Figure 4-14). At 30 K the linewidth changes abruptly and increases dramatically until the EPR signal completely disappears at approximately 18 K. The behavior is characteristic of a quasi two-dimensional magnet approaching an antiferromagnetic transition.[32,104,105] Richards and Salamon[104,105] observed similar variations in linewidths for the quasi two-dimensional K_2MnF_4 solid and Pomerantz[32] observed a similar behavior in manganese stearate films. The linewidth temperature dependence indicates the coherence length of the short-range antiferromagnetic order is increasing at lower temperatures.

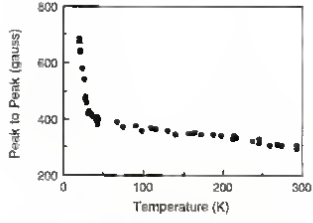

Figure 4-14. Peak to-peak width as a function of temperature.

The area of the EPR signal is directly proportional to the spin susceptibility.[32,104] In Figure 4-15 the area of the EPR signal is plotted as a function of temperature. The area increases as the temperature is lowered until a maximum value is reached at 30 K. The area then decreases rapidly. Data points taken upon cooling and heating of the LB film showed no evidence of

hysteresis. The shape of the area versus temperature plot is consistent with antiferromagnetic coupling between spins.[32,104,106] However, long range ordering is not observed due to the loss of signal. For comparison, susceptibility versus temperature data[45] for the bulk manganese phenylphosphonate is shown in Figure 4-15. The data were obtained by a SQUID magnetometer and a transition at ~ 12 K (not shown in Figure 4-15) with a T_{max} at 21 K was observed.

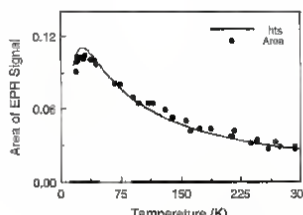

Figure 4-14. Area of the EPR signal as a function of temperature for the LB film. The solid line is fit of the data by a high temperature series expasion.[107]

The EPR intensity data from the manganese octadecylphosphonate LB film was fit with a high temperature series (hts) expansion[107] assuming that the LB film behaves as a quadratic layer Heisenberg antiferromegnet. The data was fit with the series expansion because there is no exact solution for the exchange Hamiltonian of a two-dimensional antiferromegnet[107] described as

$$\mathcal{H} = \Sigma\, J S_i \cdot S_j \qquad (4\text{-}4)$$

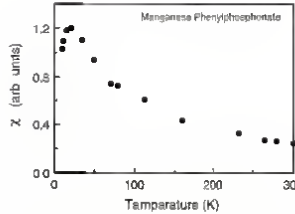

Figure 4 15 Susceptibility data for the manganese phenylphosphonate powder obtained by a SQUID magnometer

where J is the exchange constant and S is nearest neighbor spin interaction An approximate solution has been derived from a numerical series expansion [107] The simplest series expansion has been expressed for the spin susceptibility (χ) as

$$Ng^2\mu_B^2/\chi = 3\theta + \Sigma(C_n/\theta^{n-1}) \qquad (4\text{-}5)$$

where $\theta = kT/JS(S+1)$, g is the Lande factor N is the number of spins, μ_B is the Bohr magnaton and C is a coefficient. The coefficients for a S = 5/2 spin system have been calculated up to the sixth power (n = 6) [107] To solve for the susceptibility the exchange constant J is estimated from the T_{max} of the EPR data by the equation [107]

$$kT_{max}/J = 1\ 12*S(S+1) + 0\ 10 \qquad (4\text{-}6)$$

which is accurate to ± 5 percent. From the fit of the data, the exchange constant for the LB film is determined to be J/K = 3.03. The his fit is shown in Figure 4-14 along with the area versus temperature data for the EPR signal. The data fit nicely at high temperatures, but deviate somewhat near the T_{max}. The fit of the data to the two-dimensional model is further evidence for antiferromagnetic exchange in the manganese octadecylphosphonate LB film.

Summary

The use of the Langmuir Blodgett technique as a means for preparing single-layer analogs of known solid state materials has been demonstrated. The structural characterizations suggest that a multilayered film of manganese octadecylphosphonate is analogous to the manganese phenylphosphonate solid-state structure. The Langmuir-Blodgett film is a quasi-two-dimensional magnetic system. The EPR linewidth dependence as a function of orientation is consistent with the theoretical predictions for a quasi-two-dimensional material. The linewidth and area dependence as a function of temperature suggest evidence for antiferromagnetic coupling in the LB layers. The present system is different from previous attempts to observe magnetic exchange in an LB film, in that, the manganese octadecylphosphonate film forms an extended-lattice, and is a single layer analog of a known solid state structure. Future work will focus on extending the distance between planes and preparing ferromagnetic systems.

APPENDIX A
LANGMUIR-BLODGETT FILMS OF ALKYLAMMONIUM LAYERED PEROVSKITES

The alkylammonium layered perovskites [3,4,93,109] of the general formula $(RNH_3)_2MX_4$ where R is an aliphatic chain, M is a divalent metal (Cd, Cu, Cr, Mn, Fe) and X is Cl or Br, belong to a class of organic/inorganic layered materials (Figure A-1). In the crystalline state the alkylammonium layered perovskites are made up of alternating inorganic and organic layers. The inorganic layers are infinite sheets of anions of stoichiometry $(MX_4)_n^{2n-}$ with MX_6 octahedra linked in a square array by equatorial vertices.[109] The layers are seperated by layers of alkylammonium ions which maintain van der Waals contacts with one another. The NH_3^+ groups connect the organic and inorganic layers.

The alkylammonium perovskites are considered to be models for two-dimensional magnetic systems.[3,4,93,105,109] In these three-dimensional systems, the intraplane magnetic coupling is smaller than the interplane magnetic coupling, and is often ignored. We feel that a true monolayer is a more appropriate model for a two dimensional system. In a true monolayer the magnetic coupling is restricted to two-dimensions. The objective of this work is use the Langmuir Blodgett technique[10-12] to prepare a true monolayer of an alkylammonium layered perovskite and compare the magnetic properties of the monolayer to the bulk solid.

The layered perovskites are prepared by dissolving equal molar amounts of the alkylammonium chloride with the metal chloride in water followed by slow evaporation of the water.[3,4,93,109] Therefore, we propose that by incorporating

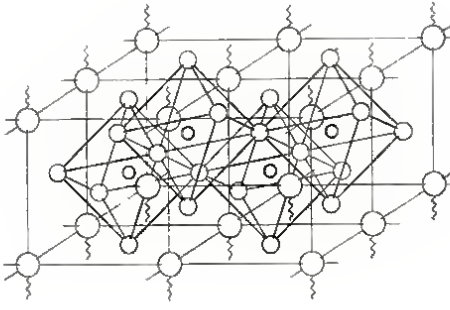

Figure A-1 The alkylammonium layered perovskite adapted from reference 108

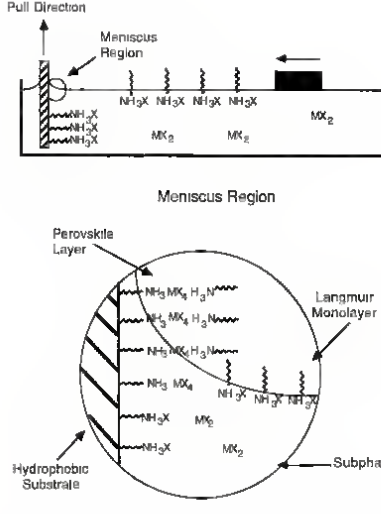

Figure A-2 Formation of a single layer of an alkylammonium perovskite using Langmuir-Blodgett deposition

the metal halide In an alkylammonium LB layer crystallization of a monolayer could occur in the meniscus region during transfer This concept is demonstrated in Figure A-2. The crystallization of the monolayer should be aided by the draining of the water from the meniscus region

Isotherms

Pressure/area isotherms are used to monitor how the subphase effects the monolayer at the air/water interface Figure A-3 compares the behavior of docosylamine on basic (NaOH) and acidic (HCl) subphases The main difference between the isotherms is that the cross-sectional area on a basic subphase is 20 5 Å^2 as compared to 28 Å^2 on an acid subphase The stability of the amine on a basic subphase is also greater than when the amine is compressed on an acidic subphase We believe that the increase in area is due to the quaternization of the amine at the air/water interface The increased stability of the amine may be attributed to the ammonium species being more soluble than the amine species In any case, it appears that the subphase has a direct effect on the floating monolayer

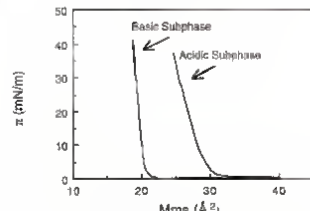

Figure A-3 Isotherms of docosylamine on a HCl and a NaOH subphase

To confirm the quaternization of the film, docosylamine was spread on a neutral subphase (Figure A 4) and compressed to a pressure of 25 mN/m. When this pressure was attained, the barrier was stopped and the decay of the film was recorded by monitoring change in π with respect to time at constant trough area. As the pressure stabilized, HCl was added to the subphase behind the barrier. The pressure began to increase until a pressure of 40 mN/m was reached. We believe that the large increase in pressure is due a close-packed amine film that is quaternized to the ammonium ion. Although it is not fully shown in Figure A-4, there is a fast decrease in pressure after the maximum pressure is reached which is consistent with the less stable floating monolayer of ammonium ions being formed at the air-water interface.

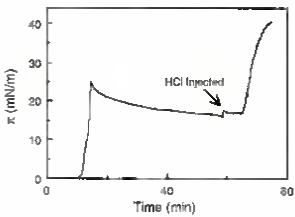

Figure A-4. Quaternization of docosylamine by injection of HCl into a neutral subphase.

Docosylamine was then compressed over a $MnCl_2$ subphase prepared at a pH = 3. We observed that an increase in $MnCl_2$ in the subphase caused an increased cross-sectional area until a constant value of 31.4 $Å^2$ was obtained. The increase in area is attributed to a Mn-complex interacting with the Langmuir

monolayer. The addition of Mn^{2+} ions also increased the stability of the film which supports the idea of incorporating ions into the film at the air/water interface.

Transferred Films

Single layer and bilayer films of docosylamine formed on a Mn-containing subphase were transferred onto hydrophilic Si substrates and hydrophobic (OTS-coated) Si substrates respectively. The transfer ratios for both single layer and bilayer films were near unity and the transfers were linear indicating that continuous films were deposited. The results from the infrared spectra are inconclusive. Table A-1 lists the IR bands that were observed in both types of films. In all cases C-H stretching bands due to the hydrocarbon chain were observed which indicates that both single layer and bilayer films were transferred; however the N-H stretches were absent. The absence of the N-H stretch is possibly due to the orientation of the N-H bond. Due to the absence of the N-H stretching bands we are unable to determine if the amine is quaternized after transfer.

Table A-1. ATR-FTIR bands for transferred LB films

Docosylamine Film	$\nu_a(CH_3)$	$\nu_s(CH_2)$	$\nu_s(CH_2)$
Monolayer	2957 cm^{-1}	2918 cm^{-1}	2850 cm^{-1}
Bilayer	2955 cm^{-1}	2915 cm^{-1}	2850 cm^{-1}

X-ray photoelectron spectroscopy (XPS) was used to analyze these films and determine the chemical species present. Table A-2 lists the chemical species present for the single layer films of docosylamine deposited from a

$MnCl_2$ subphase at pH = 3. From the data relative observed ratios can be determined using the appropriate atomic and instrument sensitivity factors [58,59]. For the single layer films the observed N:Mn:Cl ratio is 1:1:3. This suggests that the Mn complex in solution is possibly $[MnCl_3]^-$ and this complex interacts with the amine film at the air/water interface. We were able to determine that the ammonium ion is present in the transferred films by XPS. For an amine film, the binding energy of the N core electrons emitted is 406 eV[57], however, in the XPS spectrum of a single layer docosylamine film compressed on a Mn^{2+} ion subphase, the binding energy of the N core electrons is 409 ev. The increase of 3 eV in binding energy is due to a N atom in a quaternized enviroment [57]. XPS analysis of the bilayer films also showed a N:Mn:Cl ratio of 1:1:3 which is not in the correct stoichiometry for the alkylammonium layered perovskite. In order to prepare the perovskite structure the Mn complex would need to exist as $[MnCl_4]^-$ which has been observed in ethanolic or acidic medium (pH =1).[110]

Table A:2. XPS analysis of single layer docosylamine films.

Monolayer LB Film	Ions Present	Peak Area (counts-eV/s)	Ratio to N[1]
Docosylamine (acidic subphase pH = 3)	Cl	49	1
	N	37	1
Docosylamine (Mn subphase pH = 3)	Cl	918	3
	N	145	1
	Mn	1005	1

1. Ratio is derived from atomic and instrument sensitivity factors [58,59]

To date a single layer analog of the alkylammonium layered perovskites has not been prepared by the LB method. We believe that this is due to the absence of the desired metal complex ($[MnCl_4]^-$) in solution. By decreasing the pH of the subphase the $[MnCl_4]^-$ complex should be formed which is the crucial step in forming an alkylammonium perovskite monolayer.

APPENDIX B
X-RAY DIFFRACTION AND ELLIPSOMETRY

While ellipsometric results are consistent with layer-by-layer deposition of manganese octadecylphosphonate films (Chapter 4), it should be remembered that ellipsometry yields an average film thickness,[67] but does not prove that the manganese LB films possess a layered structure. Ellipsometry should be used in conjunction with other experimental data, and here the ellipsometric results are compared to grazing-angle X-ray diffraction. Figure B-1 shows grazing angle X-ray diffraction from eleven bilayers of manganese octadecylphosphonate on a silicon substrate. The deposition of the LB film was first monitored by ellipsometry (Chapter 4). Four orders of the (00*l*) reflection, including the (001), can be identified.

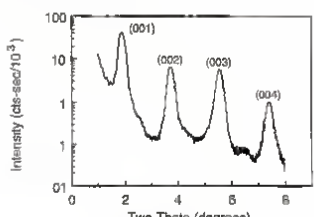

Figure B-1 Grazing angle X-ray diffraction from an eleven-bilayer manganese octadecylphosphonate LB film

The Bragg equation which is defined as

$$n\lambda = 2d(\sin\theta) \qquad \text{(B-1)}$$

where n is the order of reflection, λ is the wavelength of the X-ray, d is the distance between planes (d spacing), and θ is the angle of the incoming X-ray with respect to the surface parallel is used to calculate the distance between Mn^{2+} planes. The data correspond to a d spacing of 48.5 Å for the manganese octadecylphosphonate films which does not agree with the 53.1 Å d-spacing determined from the ellipsometric data in chapter 4. However the diffraction proves the manganese LB film is indeed layered.

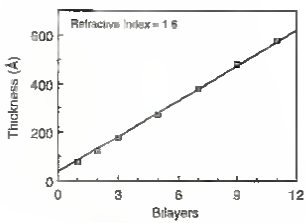

Figure B-2 Ellipsometric data for the manganese octadecylphosphonate LB film assuming a refractive index of 1.6

In these type of thin films a poor estimation of the refractive index can lead to an overestimate in film thickness.[43] It seems reasonable that the assumed refractive index of 1.54 estimated from a bulk sample may not be the

refractive index of the LB film. The refractive index of the film used for ellipsometric calculations was varied while the film thickness of 48.5 Å obtained from X-ray diffraction was held constant. Figure B-2 is a plot of the LB film thickness calculated with a film refractive index of 1.6 versus the number of LB bilayers. The film refractive index of 1.6 is consistent with a bilayer thickness of 48.5 Å.

The diffraction and ellipsometric data indicate that the refractive index of the LB film is not always the same as the bulk and that the accuracy of the ellipsometric data is dependent on the assumed refractive index of the film. However, the ellipsometric data does show a linear increase in material over a large area of the sample. It should be noted that with one-wavelength ellipsometric measurements, a two-variable equation is solved simultaneously which possibly gives rise to error in determining both thickness and refractive index of a sample.

REFERENCES

(1) *Intercalation Chemistry* Whittingham M. S., Jacobson A. J. Ed. Academic Press Inc.: New York, 1982.

(2) Cao G.; Hong H. G.; Mallouk T. E. *Acc. Chem. Res.* **1992**, *25*, 420-427.

(3) Day P. *Chem. Br.* **1983**, 306-314.

(4) Day, P. *Phil. Trans. R. Soc. Lond. A* **1985**, *314*, 145-158.

(5) Jonker, B. T.; Welker, K.; Kisker, E.; Prinz, G. A.; Carbone, C. *Phys. Rev. Lett.* **1986**, *57*, 142-145.

(6) Lowndes, D. H.; Norton, D. P.; Budai, J. D. *Phys. Rev. Lett.* **1990**, *65*, 1160-1163.

(7) Falicov, L. M. *Thin Solid Films* **1992**, *216*, 168-173.

(8) Blodgett, K. B. *J. Am. Chem. Soc.* **1935**, *57*, 1007.

(9) Langmuir, I. *J. Am. Chem. Soc.* **1917**, *39*, 1848-1906.

(10) Gaines, G. J. *Insoluble Monolayers at Liquid-Gas Interfaces*; Wiley-Interscience: New York, 1966.

(11) *Langmuir-Blodgett Films*; Roberts, G. G., Ed.; Plenum Press: New York, 1990.

(12) Ulman, A. *An Introduction to Ultrathin Organic Films: From Langmuir-Blodgett to Self-Assembly*; Academic Press: Boston, 1991.

(13) Maoz, R.; Sagiv, J. *J. Colloid Interface Sci.* **1984**, *100*, 465-496.

(14) Bain, C. D.; Troughton, E. B.; Tao, Y.-T.; Evall, J.; Whitesides, G. M.; Nuzzo, R. G. *J. Am. Chem. Soc.* **1989**, *111*, 321-335.

(15) Heywood, B. R.; Mann, S. *J. Am. Chem. Soc.* **1992**, *114*, 4681-4686.

(16) Heywood, B. R.; Mann, S. *Langmuir* **1992**, *8*, 1492-1499.

(17) Heywood, B. R.; Rajam, S.; Mann, S. *J. Chem. Soc. Feraday Trans.* **1991**, *87*, 735-743.

(18) Rajam, S.; Heywood, B. R.; Walker, J. B. A.; Mann, S.; Davey, R. J.; Birchall, J. D. *J. Chem. Soc. Feraday Trans.* **1991**, *87*, 727-734.

(19) Mann, S.; Heywood, B. R.; Rajam, S.; Birchall, J. D. *Nature* **1988**, *334*, 692-695

(20) Zhao, X. K.; Yang, J.; McCormick, L. D.; Fendler, J. H. *J. Phys. Chem.* **1992**, *96*, 9933-9939

(21) Bigelow, W. C.; Pickett, D. L.; Zisman, W. A. *J. Colloid Sci.* **1946**, *1*, 513-538

(22) Wasserman, S. R.; Tao, Y.-T.; Whitesides, G. M. *Langmuir* **1989**, *5*, 1074-1087

(23) Netzer, L.; Sagiv, J. *J. Am. Chem. Soc.* **1983**, *105*, 674-676

(24) Lee, H.; Kepley, L. J.; Hong, H.-G.; Mallouk, T. E. *J. Am. Chem. Soc.* **1988**, *110*, 618-620

(25) Lee, H.; Kepley, L. J.; Hong, H.-G.; Akhter, S.; Mallouk, T. E. *J. Phys. Chem.* **1988**, *92*, 2597-2601

(26) Akhter, S.; Lee, H.; Hong, H.-G.; Mallouk, T. E.; White, J. M. *J. Vac. Sci. Technol.* **1988**, *7*, 1608-1613

(27) Hong, H.-G.; Sackett, D. D.; Mallouk, T. E. *Chem. Mater.* **1991**, *3*, 521-527

(28) Evans, S. D.; Ulman, A.; Goppert-Berarducci, K. E.; Gerenser, L. J. *J. Am. Chem. Soc.* **1991**, *113*, 5866-5868

(29) Kepley, L. J.; Sackett, D. D.; Ball, C. M.; Mallouk, T. E. *Thin Solid Films* **1992**, *208*, 132-136

(30) Yang, H. C.; Aoki, K.; Hong, H.; Sackett, D. D.; Arendt, M. F.; Yau, S.; Bell, C. M.; Mallouk, T. E. *J. Am. Chem. Soc.* **1993**, *115*, 11855-11862.

(31) Pomerantz, M.; Dacol, F. H.; Segmüller, A. *Phys. Rev. Lett.* **1978**, *40*, 246-249

(32) Pomerantz, M. In *In NATO ASI Series*; J. G. Dash and J. Ruvalds, Ed.; Plenum: New York, 1980; pp 317-346

(33) Clearfield, A.; Smith, G. D. *Inorg. Chem.* **1969**, *8*, 431-436

(34) Alberti, G.; Costantino, U.; Allulli, S.; Tomassini, N. *J. Inorg. Nucl. Chem.* **1978**, *40*, 1113-1117

(35) Dines, M. B.; DiGiacomo, P. M. *Inorg. Chem.* **1981**, *20*, 92-97

(36) Cao G., Lee H., Lynch V. M., Mallouk, T. E. *Solid State Ionics* **1988**, *26*, 63-69

(37) Cao G., Lee H., Lynch, V. M., Mallouk T. E. *Inorg. Chem* **1988**, *27*, 2781-2785

(38) Cao G., Lynch V. M., Swinnea J. S., Mallouk T. E. *Inorg. Chem* **1990**, *29*, 2112-2117

(39) Burwell, D. A., Thompson, M. E. *Chem. Mater* **1991**, *3*, 730-737

(40) Katz, H. E., Schilling, M. L., Chidsey, C. E. D., Putvinski, T. M., Hutton, R. S. *Chem. Mater* **1991**, *3*, 699-703.

(41) Katz, H. E., Scheller, G., Putvinski, T. M., Schilling, M. L., Wilson, W. L., Chidsey, C. E. D. *Science* **1991**, *254*, 1485-1487

(42) Putvinski, T. M., Schilling, M. L., Katz, H. E., Chidsey, C. E. D., Mujsce, A. M., Emerson, A. B. *Langmuir* **1990**, *6*, 1567-1571

(43) Schilling, M. L., Katz, H. E., Stein, S. M., Shane, S. F., Wilson, W. L., Buratto, S., Ungashe, S. B., Taylor, G. N., Putvinski, T. M., Chidsey, C. E. D. *Langmuir* **1993**, *9*, 2156-2160

(44) Ungashe, S. B., Wilson, W. L., Katz, H. E., Scheller, G. R., Putvinski, T. M. *J. Am. Chem. Soc.* **1992**, *114*, 8717-8718

(45) Crewe, M. L. Masters of Science Thesis, University of Florida, 1992

(46) Byrd, H., Pike, J. K., Telham, D. R. *Thin Solid Films* **1994**, *In press.*

(47) Byrd, H., Pike, J. K., Telham, D. R. *Chem. Mater* **1993**, *5*, 709-715

(48) Ries, H. E., Jr., Cook, H. D. *J. Colloid Sci.* **1954**, *9*, 535-546

(49) Bhattacherye, A. K., Thyagarajan, G. *Chem. Rev.* **1981**, *81*, 415-430

(50) Kern, W. *J. Electrochem. Soc.* **1990**, *137*, 1887-1892

(51) Fischer, A., Sackmann, E. *J. Colloid Interface Sci.* **1988**, *112*, 1-14.

(52) Biddle, M. S., Rickert, S. E., Lando, J. B. *Thin Solid Films* **1985**, *134*, 121-134

(53) Hénon, S., Meunier, J. *Rev. Sci. Instrum.* **1991**, *62*, 936-939

(54) Siegal, S., Honig, D., Vollhardt, D., Möbius, D. *J. Phys. Chem* **1992**, *96*, 6157-6160

(55) Porter, M. D.; Bright, T. B.; Allara, D. L.; Chidsey, C. E. D. *J. Am. Chem. Soc.* **1987**, *109*, 3559-3568.

(56) Wood, K. A.; Snyder, R. C.; Strauss, H. L. *J. Chem. Phys.* **1989**, *91*, 5255-5267.

(57) *Practical Surface Analysis*, 2nd ed.; Briggs, D., Seah, M. P., Ed.; John Wiley and Sons: Chichester, MA, 1990; Vol. 2.

(58) *5000 Series ESCA Systems Version 2.0 Instruction Manual*; Perkin-Elmer Physical Electronics Division: Eden Prairie, MN, 1989.

(59) Wagner, C. D.; Davis, L. E.; Zeller, M. V.; Taylor, J. A.; Raymond, R. M.; Gale, L. H. *Surf. Interface Anal.* **1981**, *3*, 211.

(60) Seah, M. P.; Dench, W. A. *Surf. Interface Anal.* **1979**, *1*, 1-11.

(61) Poojary, M. D.; Hu, H.; Campbell, I. F. L.; Clearfield, A. *Acta Cryst.* **1994**, *In press*.

(62) Brundle, C. R.; Hopstar, H.; Swalan, J. D. *J. Chem. Phys.* **1979**, *70*, 5190-5196.

(63) Laibinis, P. E.; Bain, C. D.; Whitesides, G. M. *J. Phys. Chem.* **1991**, *95*, 7017-7021.

(64) Sastry, M.; Canguly, P.; Badrinarayanan, S.; Mandale, A. B.; Sainkar, S. R.; Paranjape, D. V.; Patil, K. R.; Chaudhary, S. K. *J. Chem. Phys.* **1991**, *95*, 6631-6635.

(65) Nesternenko, B.; Milenen, V.; Gorkun, O.; Stadnik, A.; Kazantsena, Z.; Nabok, A. *Thin Solid Films* **1991**, *201*, 351.

(66) Ohnishi, T.; Ishitani, A.; Ishida, H.; Yamamoto, N.; Tsubomura, H. *J. Phys. Chem.* **1978**, *82*, 1989-1991.

(67) Azzam, R. M. A.; Bashara, N. M. *Ellipsometry and Polarized Light*; North-Holland Publishing Co.: Amsterdam, 1977.

(68) Yamanaka, S. *Inorg. Chem.* **1976**, *15*, 2811-2817.

(69) Yamanaka, S.; Tanaka, M. *J. Inorg. Nucl. Chem.* **1979**, *41*, 45-48.

(70) Yamanaka, S.; Sakamoto, K.; Hattori, M. *J. Phys. Chem.* **1981**, *85*, 1930-1933.

(71) Tillman, N.; Ulman, A.; Schildkraut, J. S.; Penner, T. L. *J. Am. Chem. Soc.* **1988**, *110*, 6136-6144.

(72) Heller, G. L.; Rice, R. W. *J. Phys. Chem.* **1970**, *74*, 4386-4393.

(73) Garoff, S.; Deckman, H. W.; Dunsmuir, J. H.; Alvarez, M. S.; Bloch, J. M. *J. Physique* **1986**, *47*, 701-709.

(74) Inoue, T.; Yase, K.; Okada, M.; Okada, S.; Matsuda, H.; Nakanishi, H.; Kato, M. *Jpn. J. Appl. Phys.* **1989**, *28*, L2037-L2039.

(75) Reigler, J. E. *J. Phys. Chem.* **1988**, *93*, 6475-6480.

(76) Landau, E. M.; Grayer Wolf, S.; Levanon, M.; Leiserowitz, L.; Lahav, M.; Sagiv, J. *J. Am. Chem. Soc.* **1989**, *111*, 1436-1445.

(77) Landau, E. M.; Popovitz-Biro, R.; Levanon, M.; Leiserowitz, L.; Lahav, M.; Sagiv, J. *Mol. Cryst. Liq. Cryst.* **1988**, *134*, 323-335.

(78) Popovitz-Biro, R.; Lahav, M.; Leiserowitz, L. *J. Am. Chem. Soc.* **1991**, *113*, 8943-8944.

(79) Li, D.; Ratner, M. A.; Marks, T. J.; Zhang, C.-H.; Yang, J.; Wong, G. K. *J. Am. Chem. Soc.* **1990**, *112*, 7389-7390.

(80) Tillman, N.; Ulman, A.; Penner, T. L. *Langmuir* **1989**, *5*, 101-111.

(81) Frey, B. L.; Hanken, D. G.; Corn, R. M. *Langmuir* **1993**, *9*, 1815-1820.

(82) Clearfield, A. *Comm. Inorg. Chem.* **1990**, *10*, 89-128.

(83) Schoeler, U.; Tews, K. H.; Kuhn, H. *J. Chem. Phys.* **1974**, *61*, 5009-5015.

(84) Eckert, R.; Kuhn, H. *Z. Elektrochem.* **1960**, *64*, 356-364.

(85) Tasaka, S.; Katz, H. E.; Hutton, R. S.; Orenstein, J.; Fredrickson, G. H.; Wang, T. T. *Synthetic Metals* **1988**, *16*, 17-30.

(86) Cullity, B. D. *Elements of X-Ray Diffraction*; Addison-Wesley Publishing Company: Reading, CA, 1956.

(87) Swalen, J. D.; Allara, D. L.; Andrade, J. D.; Chandross, E. A.; Garoff, S.; Israelachvili, J.; McCarthy, T. J.; Murray, R.; Pease, R. F.; Rabolt, J. F.; Wynne, K. J.; Yu, H. *Langmuir* **1987**, *3*, 932.

(88) Richeson, D. S.; Tonge, L. M.; Zhao, J.; Zhang, J.; Marcy, H. O.; Marks, T. J.; Wessels, B. W.; Kannewurf, C. R. *Appl. Phys. Lett.* **1988**, *54*, 2154.

(89) de Jongh, L. J. In *Magnetic Properties of Layered Transition Metal Compounds*; L. J. de Jongh, Ed.; Kluwer Academic Publishers: Boston, 1990; pp 1-51.

(90) Mermin N D Wagner H *Phys Rev Lett* **1966** *17* 1133-1136

(91) Onsager L *Phys Rev* **1944** *65* 117-149

(92) Pokrovsky V L Uimin G V In *Magnetic Properties of Layered Transition Metal Compounds*; L J de Jongh, Ed Kluwer Academic Boston 1990 pp 53-103

(93) Arend H Tichy K Babarschka K Rys F *Solid State Commun* **1976** *18* 999-1003

(94) Krebs J J *Appl Phys A* **1989** *49* 513-521

(95) Vanderwyver M *Thin Solid Films* **1989** *159* 243

(96) Page R H Junch M C Reck B Sen A Twieg R J Swalen J D Bjorklund G C Wilson C G *J Opt Soc Am B* **1990** 1239

(97) Bellamy L J *The Infra red Spectra of Complex Molecules* 3rd ed , Chapman and Hall London 1975

(98) Thomas L C., Chittenden, R A *Spectrochim Acta* **1970** *26A* 781-800

(99) Nakamoto K *Infrared Spectra of Inorganic and Coordination Compounds* John Wiley & Sons New York 1963

(100) Byrd H Whipps S Pike J K Ma, J Nagler S E , Talham, D R *J Am Chem Soc* **1994** *116* 295-301

(101) Pike J K Byrd H Morrone A A Talham D R *J Am Chem Soc.* **1993** *115* 8497-8499

(102) de Jongh L J Miedama A R *Adv Phys* **1974** *24*, 1-260

(103) Bonosi F Gabnelli G Martini G *Colloids Surfaces A* **1993** *72* 105 110

(104) Benner H Bouchar J P In *Magnetic Properties of Layered Transition Metal Compounds*; L J de Jongh Ed Kluwer Academic. Boston, 1990 pp 323-379

(105) Richards P M Salamon M B *Phys Rev B* **1974** *9* 32-45

(106) Carlin, R L *Magnetochemistry* 1st ed , Springer-Verlag Berlin, 1986

(107) Linea M E *J. Phys. Chem Solids* **1970**, *31* 101 119

(108) Arend H Huber, W *J Cryst. Growth* **1979** *43*, 213-223

(109) Stead M J , Day P *J Chem Soc. Dalton Trans* **1982** 1081-1084

(110) Kambli U Güdel H U *Inorg Chem* **1984,** *23* 3479-3486

BIOGRAPHICAL SKETCH

Houston Byrd was born in Tampa, Florida, on September 7, 1967. After moving around the state of Florida, his family settled in Spring Hill, Florida, just before he began high school. It was in high school that Houston developed an interest in the sciences.

In the fall of 1985, Houston enrolled at Samford University located in Birmingham, Alabama. In May of 1989, he received his Bachelor of Science degree in chemistry. After graduation, he moved to Gainesville, Florida, to attend graduate school.

Houston entered graduate school at the University of Florida in the fall of 1989. By December of that year, he had joined Dr. Daniel R. Talham's research group. While at the University of Florida, he met his future wife and was married on December 19, 1992. After five years under Dr. Talham's supervision, Houston defended his dissertation and graduated from the University of Florida with a Ph.D. in chemistry.

I certify that I have read this study and that in my opinion it conforms to acceptable standards of scholarly presentation and is fully adequate in scope and quality, as a dissertation for the degree of Doctor of Philosophy

Daniel R. Talham, Chairman
Assistant Professor of Chemistry

I certify that I have read this study and that in my opinion it conforms to acceptable standards of scholarly presentation and is fully adequate in scope and quality, as a dissertation for the degree of Doctor of Philosophy

James M. Boncella
Associate Professor of Chemistry

I certify that I have read this study and that in my opinion it conforms to acceptable standards of scholarly presentation and is fully adequate, in scope and quality, as a dissertation for the degree of Doctor of Philosophy

Russell S. Drago
Graduate Research Professor of Chemistry

I certify that I have read this study and that in my opinion it conforms to acceptable standards of scholarly presentation and is fully adequate, in scope and quality, as a dissertation for the degree of Doctor of Philosophy

William M. Jones
Distinguished Service Professor of Chemistry

I certify that I have read this study and that in my opinion it conforms to acceptable standards of scholarly presentation and is fully adequate in scope and quality as a dissertation for the degree of Doctor of Philosophy

James H. Adair
Associate Professor of Materials Science and Engineering

This dissertation was submitted to the Graduate Faculty of the Department of Chemistry in the College of Liberal Arts and Sciences and to the Graduate School and was accepted as partial fulfillment of the requirements for the degree of Doctor of Philosophy

April, 1994

Dean, Graduate School